Competition of random and periodic potentials in interacting fermionic systems and classical equivalents: The Mott glass

T. Giamarchi*
Laboratoire de Physique des Solides, CNRS-UMR 85002, UPS Bat. 510, 91405 Orsay, France

P. Le Doussal† and E. Orignac‡
Laboratoire de Physique Theorique de l'Ecole Normale Superieure CNRS-UMR8549, 24 rue Lhomond, 75231 Cedex 05, Paris, France
(Received 30 April 2001; published 10 December 2001)

We study the competition between a random potential and a commensurate potential on interacting fermionic and bosonic systems using a variety of methods. We focus on one-dimensional interacting fermionic systems, but higher-dimensional bosonic and fermionic extensions, as well as classical equivalents, are also discussed. Our methods, which include the bosonization method, the replica variational method, the functional renormalization group method, and perturbation around the atomic limit, go beyond conventional perturbative expansions around the Luttinger liquid in one dimension. All these methods agree on the prediction in these systems of a phase, the Mott glass, intermediate between the Anderson (compressible, with a pseudogap in the optical conductivity) and the Mott (incompressible with a gap in the optical conductivity) insulator. The Mott glass, which was unexpected from a perturbative renormalization-group point of view has a pseudogap in the conductivity while remaining incompressible. Having derived the existence of a Mott glass phase in one dimension, we show qualitatively that its existence can also be expected in higher dimensions. We discuss the relevance of this phase to experimental systems such as disordered classical elastic systems and dirty bosons.

DOI: 10.1103/PhysRevB.64.245119 PACS number(s): 71.10.Hf, 71.30.+h

I. INTRODUCTION

In many systems, a competition between order and disorder has drastic consequences for the physical properties. Such effects are paramount when the pure system has a gap in its excitations. This situation occurs in a variety of experimental systems. The most obvious one is a Mott insulator, where interactions lead to gap in the charge excitations. Low-dimensional systems also provide many experimental situations where this competition occurs. On the theoretical side, examples include disordered spin-11 chains,[1] spin-1/2 ladders with nonmagnetic impurities,[2] disordered Mott insulators,[6,3–5] doped spin-1 chains,[7] and disordered ladder systems.[8–11] On the experimental side, examples include doped spin-Peierls systems,[12,13] and spin ladder systems.[2] However, such a phenomenon is not limited to fermionic systems. Interacting bosonic systems can also lead to a Mott insulating phase,[14–17] with which the disorder can compete. Using the standard analogy between $d+1$ classical problems and d quantum ones, it is easy to see that such a problem also encompasses elastic systems such as vortex lines in the presence of a columnar disorder.[18–20] Other pinned elastic structures such as charge-density waves[21] or spin-density waves, for which the competition between a commensurate substrate and disorder easily occurs, are also prime candidates.

In all these systems the disorder tends to close the gap. In some cases the mechanism is simple. Indeed, when the ground state is degenerate and disorder lifts this degeneracy, an infinitesimal disorder causes the formation of domains and leads to a gap closure[4] due to the Imry-Ma effect. However, in most cases the ground state is not degenerate. In this case a finite amount of disorder is needed to induce gap closure.[5] In the latter case, a complete description of the gap closure is extremely difficult, with typical analytical techniques such as a renormalization group (RG) approach, due to the absence of a weak-coupling fixed point at which the gap would close. To address this problem one has to tackle strong disorder and strong interactions simultaneously. A question of interest is of course the nature of such a transition—in particular, how one can go from an extremely ordered (gapped) phase to a (gapless) disordered one, which is known to have glassy properties, at least in high enough dimensions.

Not surprisingly, given the complexity of the problem, very little is known. In one dimension a RG study combining the RG's for pure commensurate systems[22,23] and an incommensurate disordered system[24] was performed.[5] Since both the commensurate potential (umklapp) and the disorder are relevant operators, no controlled analysis of the transition could be done. It was inferred from these studies that one goes from a Mott phase to a disordered phase (Anderson) depending on which operator became relevant first. The idea of a direct Mott-Anderson transition seemed the most natural one, and was the one usually assumed in the literature. Solutions on a special point (Luther-Emery line) also supported such conclusions.[3]

In the present paper we reexamine this problem. For fermionic systems it is of course difficult to tackle the interactions in general, so we will mostly focus on the one-dimensional case where the interactions can be handled via the bosonization technique. This allows us to derive a phase Hamiltonian that makes a connection between this problem and disordered elastic problems. A study of this phase Hamiltonian using better suited methods that capture some nonperturbative effects—(i) an atomic limit, (ii) a variational method, and (iii) a functional renormalization-group method—allows one to reach the consistent conclusion that the transition between the Mott insulator and the Anderson

phase (that we call Anderson glass to emphasize its glassy properties) *is not direct*. An intermediate phase, which has a gap in some of its excitations and yet is glassy, does exist. We determine the characteristics of this phase, that we call the Mott glass (MG) phase. Since the phase Hamiltonian does describe quantum crystals and bosons in arbitrary dimensions, but interacting fermions only in one dimension, we also give an excitonic argument directly for fermions that indicates that this phase also exists for fermionic systems in dimensions greater than 1. Some of these results were presented in a shorter form in Ref. 25.

The plan of the paper is as follows. In Sec. II we introduce fermionic models for disordered Mott systems. We then show in Sec. II B how in one dimension this model reduces, using bosonization, to a phase Hamiltonian that will be the core of our study. Section II C links this phase Hamiltonian with the other quantum crystals and classical disordered elastic systems for which our study is relevant. Section III is devoted to an analysis of this phase Hamiltonian, using an atomic limit (Sec. III A), a variational method (Sec. III B) and a functional renormalization-group study (Sec. III C). We show the existence of the Mott glass phase which is both incompressible and glassy. A reader interested only in the physical properties of the MG phase can skip these relatively technical sections and go straight to Sec. IV, where we examine in detail the physical properties (correlations functions, transport, etc.) Since the link between the phase Hamiltonian and the interacting fermions only exists in $d=1$, we directly examine the fermions in higher dimensions in Sec. IV B, and give an atomic limit argument showing that the physics of the Mott glass phase exists regardless of the dimension. Finally the conclusions can be found in Sec. V. Some technical details are pushed to the appendixes of the paper.

II. MODELS AND PHYSICAL OBSERVABLES

A. Interacting fermions

We want to study the competition between a Mott insulator and an Anderson insulator in a dirty fermion system at commensurate filling. The prototype model for this problem is the extended Hubbard model with a random on-site potential at half-filling,

$$H=-t\sum_{\langle i,j\rangle\sigma}(c^{\dagger}_{i,\sigma}c_{j,\sigma}+\text{H. c.})+U\sum_i n_{i,\uparrow}n_{i,\downarrow}+V\sum_{\langle i,j\rangle}n_i n_j+\sum_i W_i n_i, \tag{1}$$

where $\langle,\rangle$ denotes a sum over nearest neighbors, σ is the spin, and $n_i=n_{i\uparrow}+n_{i\downarrow}$ is the total fermion number on site i. W_i is the random potential at site i. For reasons that will become clear we also include a nearest-neighbor repulsion V. A general discussion of the physics of this model will be given in Sec. IV. Given the complexity of this model, let us first examine a much simpler situation in which explicit calculations can be performed.

B. Interacting fermions in $d=1$ and bosonized Hamiltonian

In one dimension, many simplifications occur. Indeed, in one dimension, it is possible to reexpress Hamiltonian (1) in terms of the collective charge and spin excitations of the system. This procedure is by now standard in one dimension, and we refer the reader to Refs. 26–29 for more details. In terms of the bosonic charge ϕ_ρ and spin ϕ_σ collective variables, (1) becomes

$$H=H_\rho+H_\sigma+H_W, \tag{2}$$

$$H_\rho=\hbar\int\frac{dx}{2\pi}\left[u_\rho K_\rho(\pi\Pi_\rho)^2+\frac{u_\rho}{K_\rho}(\partial_x\phi_\rho)^2\right]+\frac{2g_3}{(2\pi a)^2}\int dx\cos\sqrt{8}\phi_\rho, \tag{3}$$

$$H_\sigma=\hbar\int\frac{dx}{2\pi}\left[u_\sigma K_\sigma(\pi\Pi_\sigma)^2+\frac{u_\sigma}{K_\sigma}(\partial_x\phi_\sigma)^2\right]+\int dx\frac{2g_{1\perp}}{(2\pi a)^2}\cos\sqrt{8}\phi_\sigma, \tag{4}$$

$$H_W=\int dx W(x)\rho(x), \tag{5}$$

where $\rho(x)$ is the continuum limit of the charge density and reads

$$\rho(x)=-\frac{\sqrt{2}\partial_x\phi_\rho}{\pi}+\frac{1}{(2\pi\alpha)}[e^{i\sqrt{2}\phi_\rho-2k_F x}\cos\sqrt{2}\phi_\sigma+\text{H.c.}]+\tilde{\rho}_0\cos(\sqrt{8}\phi_\rho-4k_F x). \tag{6}$$

Here $\tilde{\rho}_0$ and is the renormalized amplitude, and α is a length of the order of the lattice spacing. All microscopic interactions are absorbed in the Luttinger parameters u_ρ and K_ρ. Spin rotation symmetry leads to $g_{1\perp}=0$ and $K_\sigma=1$ at low energy. For very repulsive interactions ($K_\rho<1/3$) the $4k_F$ density fluctuations are the most relevant, as can be seen[30] from Eq. (6). In this limit,[31] spin fluctuations suppress the $2k_F$ part of the density fluctuations with repect to the $4k_F$ part. Let us note that such a limit cannot be achieved within a pure Hubbard model with only on-site interactions. However, it can be achieved within an extended Hubbard model with interactions of finite range.[31–33] Thus one can study a Hamiltonian containing only charge degrees of freedom:

$$H=\int\frac{dx}{2\pi}\hbar u_\rho\left[K_\rho(\pi\Pi_\rho)^2+\frac{(\partial_x\phi_\rho)^2}{K_\rho}\right]-\frac{g}{\pi\alpha}\int dx\cos\sqrt{8}\phi_\rho+H_W. \tag{7}$$

One can perform the rescaling $\phi=\sqrt{2}\phi_\rho$ and $\Pi=\Pi_\rho/\sqrt{2}$, which leads to the action where we have introduced $v=u_\rho$, $K=K_\rho$:

$$\frac{S}{\hbar}=\int dx\int_0^{\beta\hbar}d\tau\left\{\frac{1}{2\pi K}\left[\frac{(\partial_\tau\phi)^2}{v}+v(\partial_x\phi)^2\right]-\frac{g}{\pi\alpha\hbar}\cos 2\phi+H_W\right\}. \quad (8)$$

Hamiltonian (7) also describes interacting one-dimensional *spinless* fermions in a commensurate periodic plus random potential. The lattice form of such a model is

$$H=-t\sum_i\ (c_i^\dagger c_{i+1}+\text{H. c.})+\sum_i\ [W_i+g\cos(2k_F ia)]c_i^\dagger c_i+V\sum_i\ n_i n_{i+1}, \quad (9)$$

where $\overline{W_iW_j}=D\delta_{ij}$, and k_F is the Fermi wave vector of the spinless fermions system. In the continuum Eq. (9) leads to

$$H=-i\hbar v_F\int dx(\psi_R^\dagger\partial_x\psi_R-\psi_L^\dagger\partial_x\psi_L)+V\int dx\rho(x)^2-g\int dx(\psi_R^\dagger\psi_L+\psi_L^\dagger\psi_R)+\int dxW(x)\rho(x). \quad (10)$$

g measures the commensurate potential, V the interaction, and D the disorder strength. Upon bosonization, Hamiltonian (10) becomes Eq. (7). One can thus see that in one dimension, there is no essential difference in the charge sector between a band insulator (with a $2k_F$ periodic potential) and a Mott insulator (which can be viewed as a system in a $4k_F$ periodic potential[17]). We stress that, in order to establish the equivalence of the bosonized charge sector of Hamiltonian (1) and the bosonized representation of Hamiltonian (9), one does not rely on the equivalence of charge excitations of the Hubbard model in the limit $U/t\to\infty$ with spinless fermions.

1. Random potential

Let us now qualitatively describe the effect of the various components of the random potential. The effects of disorder on a dimensional *noninteracting* system are well known.[34,35] Disorder, however, weakly localizes all electronic states leading to an insulating behavior. However, contrary to what happens in the case of a periodic potential, there is no gap at the Fermi level but a finite density of states. Also, the ac conductivity does not show a gap but a behavior of the form $\sigma(\omega)\sim\omega^2$ up to logarithmic corrections. In the presence of interactions, disorder can be treated by bosonization. For weak disorder, in the random potential one can separate the Fourier components close to $q\sim 0$ (forward scattering or random chemical potential) and $q\sim 2k_F$ (backward scattering) as

$$W(x)=\mu(x)+\xi(x)e^{2ik_Fx}+\xi^*(x)e^{-i2k_Fx}, \quad (11)$$

and treat them separately. Hamiltonian (7) becomes, for $g=0$,

$$H_{\text{dis}}=\int dx\frac{\hbar v}{2\pi}\left[K(\pi\Pi)^2+\frac{(\partial_x\phi)^2}{K}\right]-\int dx\mu(x)\frac{1}{\pi}\partial_x\phi(x)+\int dx\frac{\xi(x)}{2\pi\alpha}e^{i2\phi(x)}+\text{H.c.}, \quad (12)$$

where $\overline{\mu(x)\mu(x)}=D_f\delta(x-x')$ and $\overline{\xi(x)\xi^*(x')}=D_b\delta(x-x')$ and $D_f=D_b=W$.

The random chemical potential μ can be absorbed[24] in the quadratic part of Hamiltonian (12) by performing the transformation

$$\phi(x)\to\phi(x)+\frac{K}{\hbar v}\int^x\mu(x)dx. \quad (13)$$

Therefore, this term has no role in Anderson localization in the interacting system, in analogy with the noninteracting case.[35] The backward scattering ξ causes Anderson localization. Using the renormalization-group approach[36,24] it is easy to see that ξ is relevant for not too attractive interactions $K<3/2$, and becomes of order 1 at a length scale

$$l_0=\alpha\left(\frac{\hbar^2v^2}{16W\alpha K^2}\right)^{1/(3-2K)}, \quad (14)$$

identified as the localization length in the interacting system. Beyond this length l_0, the phase ϕ becomes random and all correlations decay exponentially.

2. Disorder and commensurate potential

In the absence of disorder a commensurate potential leads to a gap opening for $K<2$. When disorder is added to such a commensurate phase, its various Fourier components should be distinguished. Both forward and backward scatterings can compete with the commensurate potential, but, as we have seen above, they can lead to quite different types of ground states. The most interesting case is the competition of the commensurate potential with the backward scattering.

In order to understand the competition between the commensurate potential and the backward scattering, one can argue that the phase physically realized will be the one with the shortest correlation length. For the Mott phase the relevant length is the Mott length d, which is the inverse of the gap, or the size of a charge soliton. Thus, if $d<l_0$, one could expect the system to be a gapped Mott insulator, whereas for $l_0<d$ the gap would be washed out by disorder and the system would be in the Anderson insulating phase. This qualitative argument can be put on a more formal basis by writing perturbative RG equations for the coupling constant g of the commensurate potential and the disorder potential W. Both the pure commensurate case and the disordered incommensurate case lead to runaway flow where the coupling constant (g or W) reach strong coupling (at lengths d or l_0). A naive extrapolation consists of assuming that the phase that is physically realized is the one for which the coupling constant reaches strong coupling first. Based on such an extrapolation of the RG analysis,[5] one thus expects a single transition between a commensurate (incompressible) phase and an Anderson (compressible) insulator. In order to go beyond this un-

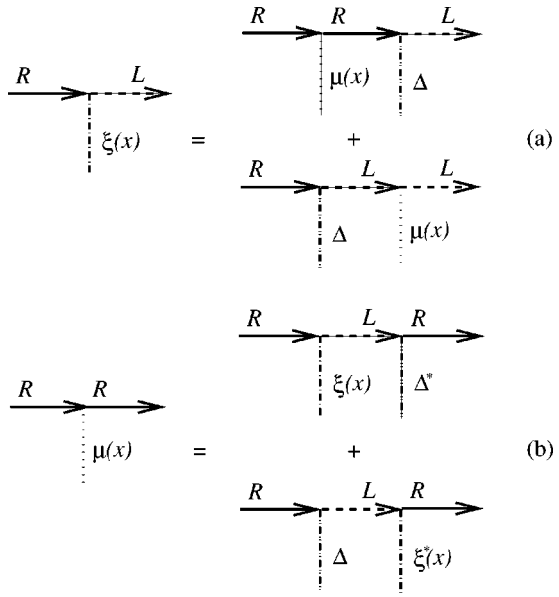

FIG. 1. The generation of effective backward (a) and forward (b) scattering from forward (backward) scattering and commensurate potential. μ and ξ, respectively, denote the forward and backward parts of the random potential (see text), and g the commensurate potential. R and L, respectively, denote right- and left-going fermions with a momentum close to $+k_F$ $(-k_F)$.

controlled extrapolation to the strong coupling of the RG results, in this paper we will use several nonperturbative methods.

Note that a complication arises from the fact that in the presence of an commensurate potential, a forward (backward) random potential is generated by the backward (forward) component, as shown in Fig. 1. So, in principle, these two components of the disorder should not be treated separately. However, for $K>3/2$ the backward scattering is irrelevant, so one can focus on forward scattering alone. On the other hand, in the limit of strong repulsion, it can be shown that the closure of the gap that would be induced by a purely forward potential would occur at much stronger disorder than the one caused by a purely backward disorder (see Appendix A). It is thus reasonable to expect that in the limit of strong repulsion, and for a backward disorder of the same order of magnitude as the forward disorder, the closure of the Mott gap is to be attributed to the backward component of the disorder. This allows one, in the limit of strong repulsion, to neglect the forward component of disorder altogether. Since in the following we will consider only this case, we will be justified in dropping the forward component. A detailed treatment of the forward scattering can be found in Appendix A.

C. Other quantum and classical elastic systems

Besides interacting fermions in one dimension, the phase model describes many other physical systems both in one dimensionl and higher dimension. It is easiest to discuss it in the Lagrangian path-integral formulation. To fix notations let us first generalize the imaginary time quantum action [Eq. (8)] [entering into the path integral in $(d+1)$ dimensions as $\int D\phi e^{-S/\hbar}$] to an arbitrary dimension d as follows:

$$\frac{\mathcal{S}}{\hbar}=\int_0^{\beta\hbar} d\tau \int d^dx\left[\frac{v}{2\pi K}(\partial_x\phi)^2+\frac{1}{2\pi vK}(\partial_\tau\phi)^2+\frac{V_p(\phi(x))}{\hbar}+\frac{V(\phi(x,\tau),x)}{\hbar}\right], \tag{15}$$

with $\overline{V(\phi,x)V(\phi',x')}=\delta(x-x')R(\phi-\phi')$. The bare disorder correlator and bare periodic potential can be chosen as $R(\phi)=W/[2(\pi\alpha)^2]\cos 2\phi$ and $V_p(\phi)=-g/(\pi\alpha)\cos(2\phi)$, respectively, although higher harmonics, preserving the π periodicity, *do appear* under coarse graining and play an important role (even in $d=1$).

Before proceeding, and since the *classical limit* of this quantum action will be of importance below, let us note that it is obtained by letting $\hbar\to 0$, and $K\to 0$, $\overline{K}=K/\hbar$ fixed, with β fixed, the zero temperature limit $\beta\to+\infty$ (of interest here) being taken *at the end* (this can be seen, e.g., by rescaling $\tau=\hbar\tau'$ so as to keep the bound of integrations fixed as $\hbar\to 0$). There are two types of systems which can be described by Eq. (15): quantum elastic systems with point disorder and classical equivalent systems with *correlated disorder* as we now describe.

1. Quantum crystals with point disorder

Let us consider a quantum crystal in dimension d in a commensurate periodic potential plus a random potential. In this case, each particle can be described by its displacement with respect to its equilibrium position $u(x)$, and the associated phonon modes. In general the displacement field has N components, with $N=d$ for crystals of bosons or fermions, $N=2$ and $d=3$ for a crystal of vortex lines, etc. At $T=0$, the system can still have quantum fluctuations, leading to a quantum crystal (for a review see Ref. 37). Examples of quantum crystals to which our present study can apply are charge-density-wave crystals,[21] electron Wigner crystal,[38,39] electrons at the surface of helium $(d=2)$, stripes in oxides. Other systems with $N<d$ such as, e.g., a vortex lattice at temperature low enough such that quantum fluctuations of vortices become important, can also be studied. In this case a periodic potential also exists from the underlying crystal, or for layered superconductors when the field is applied parallel to the layers.

The Hamiltonian of such system can be written as

$$H=H_0+H_P+H_W. \tag{16}$$

The harmonic part of the Hamiltonian of the system then reads

$$H_0=\frac{1}{2}\int d^dx\left[\frac{\Pi_i\Pi_i}{2M}+C_{ij}^{kl}\partial_{x_i}u_k\partial_{x_j}u_l\right], \tag{17}$$

where $x=(x_1,\ldots,x_d)$, C_{ij}^{kl} is an elastic matrix, and Π_i are the momenta. The particle density can be written as the sum[40]

$$\rho(x)=\sum_R \delta(x-R+u(R))=\rho_0\sum_G e^{iG\cdot[x-u(x)]} \quad (18)$$

over all reciprocal-lattice vectors G, and $u=u_1,\ldots,u_d$. This allows one to write the periodic part of the Hamiltonian as

$$H=\int d^dx\sum_G V_G e^{iG\cdot u(x)}, \quad (19)$$

and the disorder part of the Hamiltonian as

$$H=\int d^dx\sum_G W_G(x)e^{iG\cdot u(x)}. \quad (20)$$

To minimize technicalities we will not explicitly study the general case of an arbitrary lattice, but a simpler $N=1$ version where one keeps only one component to the displacement field u. In addition to already being a good approximation in some cases (i.e., keeping only the transverse displacement and its associated shear modulus in a two-dimensional lattice) the general case is rather similar up to algebraic complications related to the tensor structure. Thus a quantum crystal with point disorder and commensurate potential can be modeled by quantum action (15) with the correspondence $\phi(x)=\pi u(x)/a$, where a is the lattice spacing, and $1/2a^2v\bar{K}$ the elastic coefficient. We refer the reader to Refs. 38 and 39 for more detailed descriptions for $N>1$.

2. Equivalent classical systems with correlated disorder

A $(d+1)$-dimensional classical elastic system in presence of correlated disorder and periodic potential is described at a temperature T_{cl} by its partition sum

$$Z_{cl}=\int D\phi e^{-H_{cl}/T_{cl}}, \quad (21)$$

$$\frac{H_{cl}}{T_{cl}}=\frac{1}{2T_{cl}}\left[\int_0^L dz\int d^dx c(\partial_x\phi)^2+c_{44}(\partial_z\phi)^2+V_p[\phi(x,z)]+V[\phi(x,z),x]\right], \quad (22)$$

where $\phi(x,z)$ is a deformation field and L a thickness in the direction of correlation. For a system with internal periodicity, such as a classical crystal or a classical charge-density-wave (CDW) crystals, one has $2\phi=2\pi u/a$, a being the lattice spacing and $u(x,z)$ the $N=1$ displacement field. In this case the disorder $V(\phi,x)$ and periodic modulation (i.e., the density for a crystal) have the same periodicity as given above. A prominent example is the flux line lattice in superconductors (which has $N=2$) in the presence of columnar defects. c and c_{44}, respectively, are then proportional to the bulk (or shear) and tilt modulus.

The two problems, i.e., Eqs. (22) and (15), are thus directly related via the correspondences

$$z=\tau,$$

$$L=\beta\hbar,$$

$$T_{cl}=\hbar,$$

$$c_{44}=\frac{1}{\pi v\bar{K}},$$

$$c=\frac{v}{\pi\bar{K}}, \quad (23)$$

with $\bar{K}=K/\hbar$. The two equivalent models can thus be studied simultaneously. The classical limit of the d-dimensional quantum model corresponds to the zero-temperature limit of the $d+1$ equivalent classical model. Note that the boundary conditions may differ: periodic for quantum particles (antiperiodic for fermions), but usually free for a classical system (unless artificially considered on a torus). Also note that another correspondence could be defined with $L=\beta$ and $z=\tau/\hbar$.

III. STUDY OF THE PHASE MODEL

In this section we study the phase model. Before embarking on the heavy machinery of the replica variational method (in $d=1$) and of the functional RG method (in a $d=4-\epsilon$ expansion), we first show how the three phases of the model can be obtained very simply in the following *double limit*: (i) classical limit and (ii) atomic limit. Perturbations around those limits can then be done, and this is not expected to yield drastic changes, as confirmed by more sophisticated methods below.

A. Phase diagram from the atomic limit

In this section we focus on the *classical limit* of model (15), i.e., $\hbar\to 0$, $K\to 0$ with $\bar{K}\sim K/\hbar$ and β fixed and further consider the zero temperature limit by taking $\beta\to+\infty$ *at the end*. We also perform the rescaling $\phi\to\phi/2$ to simplify the equations. As will be shown in the following, the phases identified here survive at small enough $K>0$ for $d\geqslant 1$. Indeed perturbations away from this limit are irrelevant in the RG sense. As is well known, the classical version is still nontrivial since there is still a competition between the commensurate potential and disorder on one hand and the elastic term which produces a nontrivial classical configuration satisfying

$$\frac{\delta S}{\delta\phi^0(x)}=-\frac{v}{4\pi\bar{K}}\nabla_x^2\phi^0(x)+\frac{1}{\pi\alpha}[g\sin(\phi^0(x)]+v(x)\cos[\phi^0(x)-\zeta(x)]=0, \quad (24)$$

where we define $\xi(x)^*/(\pi a)=iv(x)e^{i\zeta(x)}$. There may be several solutions to this equation [apart from the global periodicity $\phi^0(x)\to\phi^0(x)+2m\pi$], but the physically relevant ones that we consider here are the ones with lowest energy (or action $S[\phi^0]$), which are selected as $\hbar\to 0^+$.

We now consider the additional limit $1/\bar{K}\to 0$, called the atomic limit because the model effectively becomes zero dimensional in this limit. In a second stage we describe the

deviations from the atomic limit. We assume everywhere that the disorder is *bounded* which turns out to be of some importance, the case of Gaussian disorder being discussed below.

1. Atomic model: $\bar{K}^{-1}=0$

Dropping the elastic term in Eq. (24), we are thus left to study the $d=0$ model Hamiltonian in the classical limit,

$$H_1(\phi)=-v\cos(\phi-\zeta)-g\cos(\phi), \tag{25}$$

with ζ a random phase distributed uniformly in $[0,2\pi]$, and v a random variable which we choose to have a *bounded support* $-W<v<W$. In the absence of disorder the minima are at $\phi=2\pi n$. In the presence of disorder this model has (up to the periodicity $\phi\to\phi+2\pi n$) a unique local (and global) minimum with probability 1 for all parameters. Indeed, one can rewrite

$$H_1(\phi)=-\alpha\cos(\phi-\zeta'), \tag{26}$$

$$\alpha=\sqrt{v^2+2vg\cos(\zeta)+g^2}, \tag{27}$$

$$\alpha e^{-i\zeta'}=g+ve^{-i\zeta}, \tag{28}$$

and thus there is a single minimum (for $\alpha>0$) at $\phi_0=\zeta'$.

An interesting change of behavior occurs, however, at $W=g$. For $W<g$ the distribution of α is bounded away from 0, with $g-W<\alpha<W+g$, and another minimum is distributed in the interval $-\phi_{max}<\zeta'<\phi_{max}$ with $\sin(\phi_{max})<W/g$. For $W>g$, α is distributed in the interval $0<\alpha<W+g$ and thus can take values arbitrarily close to zero. Simultaneously, the minimum position ζ' is now distributed in all of $[0,2\pi]$.

Thus in this simple model two things happen simultaneously as the disorder width W increases beyond $W=g$. First the distribution of the Hessian eigenvalue $H''(\phi_0)=\alpha$ extends down to 0 (while it is bounded away from zero for weaker disorder). Second, the probability distribution of ϕ_0 changes abruptly at $W>g$ (while it is bounded in a subinterval of $[-\pi/2,\pi/2]$) below. As will become clear below, this abrupt change of behavior corresponds to a direct transition from Mott insulator to Anderson glass phases, which is in fact a multicritical point in the $\hbar=0$ phase diagram.

It turns out that the above form for $H_1(\phi)$ does not yield a generic behavior for $d=0$. This can easily be seen by adding higher harmonics, and we will illustrate it by simply adding a small second harmonic to the disorder. It must be stressed that these higher harmonics are always generated in perturbation theory beyond the atomic limit (see, e.g., Sec. III C) and that they are generically present in realistic models and should thus be included. Thus we now study

$$H_2(\phi)=-v\cos(\phi-\zeta)-v_2\cos(2\phi-2\zeta_2)-g\cos(\phi), \tag{29}$$

with ζ_2 another random phase uniform in $[0,2\pi]$ independent of ζ. One can rewrite

$$H_2(\phi)=\alpha[\cos\psi+\beta\cos(2\psi-2\chi)], \tag{30}$$

$$\psi=\phi-\zeta', \tag{31}$$

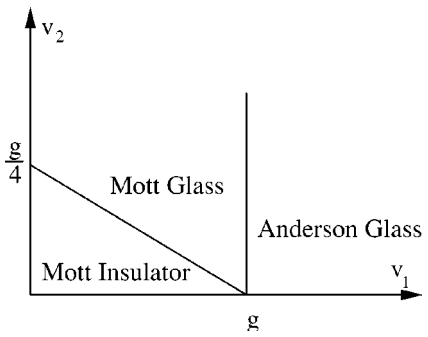

FIG. 2. Phase diagram in the atomic limit: v_1 and v_2 are the disorder strengths of the two disorder harmonics, and g is the strength of the commensurate potential. The three different phases are MI, which has a unique local minima with probability 1; MG, which corresponds to a nonzero probability to have two local minima and a zero probability that any minima lie outside of $]-\pi/2,\pi/2[$; and AG, which has a nonzero probability to have two local minima and a finite probability that minima are outside of $]-\pi/2,\pi/2[$ (and thus that there are kinks; see the text).

$$\beta=v_2/\alpha,\quad \chi=\zeta_2-\zeta', \tag{32}$$

and α and ζ' as above. Note that χ is still uniform in $[0,2\pi]$. Let us consider a fixed β. It is easy to see that for $\beta<1/4$ there is a unique minimum for any value of χ, and the situation is similar to the one discussed above. But, as soon as $\beta>1/4$, there is a value of χ for which *there is a second minimum*. At $\beta=1/4^+$ the second minimum appears for $\chi=0$. Thus interesting things happen in this model. The phase diagram is shown in Fig. 2. Let us consider, for simplicity, the case where $v_1\equiv v$ and v_2 are fixed and positive and only the phases are random (the general case is similar). There are three phases in this simple, exactly solvable, model.

(i) For $v_1<g$, α is bounded from below ($\alpha>g-v_1$) and for small enough $v_2<\frac{1}{4}(g-v_1)$ a *single minimum* exists: this corresponds to the Mott insulator (MI) phase shown in Figs. 3 and 4.

(ii) For $v_1<g$ and $v_2>\frac{1}{4}(g-v_1)$ *two minima exist*. This corresponds to the MG phase. Just above the line $v_2=\frac{1}{4}(g$

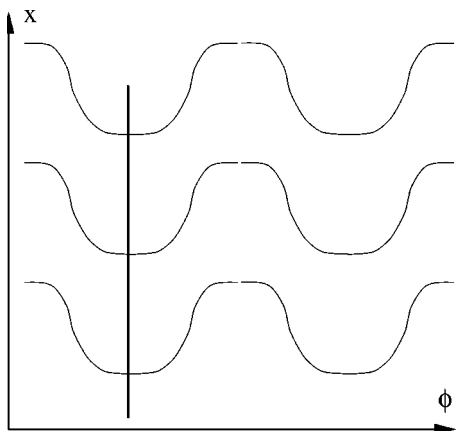

FIG. 3. Pure Mott insulator phase without disorder. A ground state in the classical limit $\phi_0(x)=0$ is represented.

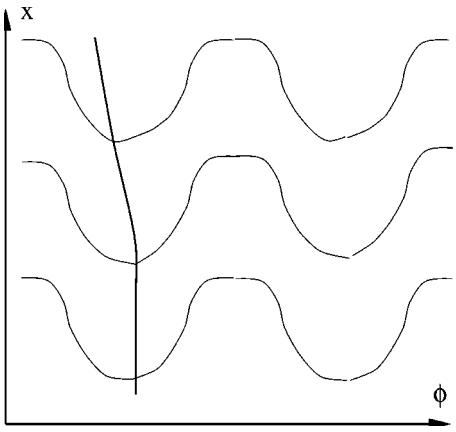

FIG. 4. *Mott insulator phase* with disorder. The ground state in the classical limit $\phi_0(x)$ is represented. It is only slightly deformed with respect to $\phi_0(x)=0$. No other local minima exists (up to the global periodicity $\phi_0(x)\to\phi_0(x)+2\pi$). The stability eigenvalues of the Hessian matrix at $\phi_0(x)$ are strictly positive, and bounded from below by a positive number m_R^2. There is a gap $\sim m_R^2$ in the conductivity. The compressibility is still zero, since the response to a tilt $h\partial_x\phi$ vanishes as no kinks exist.

$-v_1$), the equilibrium positions are $\psi=\chi\approx 0$, $\phi_0\approx\zeta'$, and $|\phi_0|<\phi_m<\pi/2$ with $\sin\phi_m=v_1/g$. Thus, with a probability as exactly 1, the two minima remain in the wells of the original cosine, i.e., the probability that the second minimum is outside of the interval $[-\pi/2,\pi/2]$ is exactly zero. This is represented in Fig. 5.

(iii) For $v_1>g$, α has a finite probability to be arbitrarily close to zero, and one easily sees that the probability of having two minima is nonzero and the probability that the second minimum is outside of the interval $[-\pi/2,\pi/2]$ is nonzero. This phase corresponds to the Anderson glass, as shown on Fig. 6.

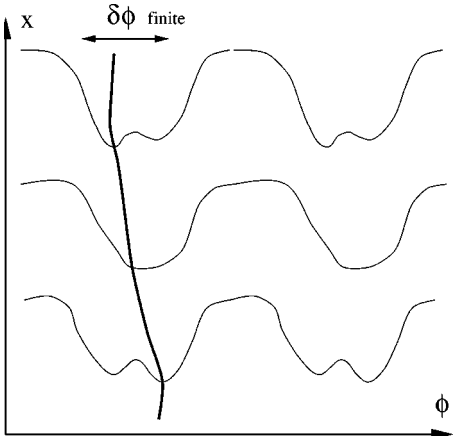

FIG. 5. *Mott glass phase*: the ground state in the classical limit $\phi_0(x)$ is represented. Other metastable states exist, and the stability Hessian matrix at $\phi_0(x)$ spectrum extends down to 0. There is no gap in the conductivity. The wandering of the ground state along x is bounded as $|\phi_0(x)-\phi_0(x')|$ is finite (and the x averaged positions is at $\phi=0$). The compressibility is still zero, since the response to a tilt $h\partial_x\phi$ (i.e., a change in chemical potential) vanishes as no kinks exist between the well-separated original minima of the cosine $\phi=2n\pi$.

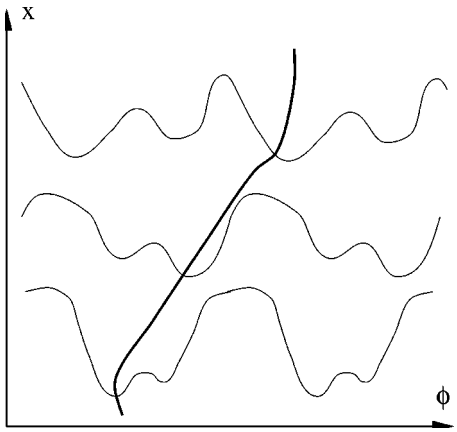

FIG. 6. *Anderson glass phase*: the ground state in the classical limit $\phi_0(x)$ is represented. Many other metastable states exist, and the stability Hessian matrix spectrum extends down to 0. There is no gap in the conductivity. The wandering of the ground state along x, $|\phi_0(x)-\phi_0(x')|$, is unbounded. The compressibility is nonzero as the ground state reorganizes in response to a tilt $h\partial_x\phi$ (i.e., a change in chemical potential) because kinks of energies arbitrary close to zero now exist.

2. Expansion around the atomic limit, d≥1

We can now expand around the atomic limit and consider a large but finite $\overline{K}$. Let us consider $d=1$ for simplicity, but similar arguments apply to any $d\geq 1$. We must construct the classical configuration of the Hamiltonian,

$$H(\phi)=\int_x \frac{c}{2}(\nabla_x\phi)^2-v\cos[\phi(x)-\zeta(x)] - v_2\cos[2\phi(x)-2\zeta_2(x)]-g\cos[\phi(x)], \quad (33)$$

with $c=v/\pi\overline{K}$. Assume again for simplicity that v and v_2 constants. Let us work in the limit of elastic coefficient c very small [large but finite $\overline{K}$, or equivalently a long correlation length for the independent random phases $\zeta(x)$ and $\zeta_2(x)$]. Then we can think of the model as a succession along x of $d=0$ models (slices) with different realizations of the disorder, and consider, e.g., a discretized version

$$H(\phi)=\sum_n \frac{c}{2}(\phi_{n+1}-\phi_n)^2-v\cos(\phi_n-\zeta_n) - v_2\cos(2\phi_n-2\zeta_{2,n})-g\cos(\phi), \quad (34)$$

where ζ_n and $\zeta_{2,n}$ are independent from slice to slice.

Let us think of a formal perturbation in the elastic coefficient c. For $c=0$ we know the minima for each slice, analyzed above, noted by $\phi_0^n+2\pi k_n$. For $c>0$, one easily sees that to lowest (naive) order in c, to construct a minimal energy configuration one must first choose which minima of successive slices to connect together. The small shifts in minima positions and the ensuing changes in minima energies are formally of higher order [they become relevant in the MG and Anderson glass (AG) phases, and are discussed below but they do not change our main argument here]. Thus at each x slice we must choose whether to connect ϕ_0^n to

ϕ_0^{n+1} (defined as the minimum in $[-\pi,\pi]$ of the corresponding $d=0$ model) or to $\phi_0^{n+1}\pm 2\pi$ (which we call a kink). This is equivalent (formally to lowest order in c) to choosing iteratively the one of the three minima which minimizes the distance $\min_{m=0,1,-1}(|\phi_0^n-\phi_0^{n+1}+2m\pi|)$. The way these minima are connected define the three phases.

(i) In the MI regime defined above ($v_1<g$, $v_2<(g-v_1)/4$) connecting the minima is obvious, and leads to a typical ground state as represented in Fig. 4, which defines the MI phase.

(ii) In the MG regime ($v_1<g$, $v_2>(g-v_1)/4$) the key observation is that connecting the minima remains *unambiguous* thanks to the fact that the distribution of the position of these minima remains confined with probability 1 within $[-\phi_m,\phi_m]$ with $\phi_m<\pi/2$. Indeed, as long as $\phi_m<\pi/2$ the distance for a kink $|\phi_0^n-\phi_0^{n+1}\pm 2\pi|>2\pi-2\phi_m$ is always larger than $2\phi_m$ the distance to connect two minima maximally separated. Thus the elastic energy always penalizes the kinks. One thus finds that the string ϕ_0^n will remain confined, for small c, within the interval $[-\phi_m',\phi_m']$ with $\phi_m'<\pi/2$. This is represented in Fig. 5, and corresponds to the Mott glass phase.

(iii) In the AG regime ($v_1<g$), in each $d=0$ slice ϕ_0^n can be in any position of $[-\pi,\pi]$. Thus connecting the minima becomes qualitatively (although not quantitatively) the same problem as for a standard CDW crystal without the periodic potential. This is the Anderson glass phase.

Thus these semirigorous arguments show that the three phases which already exist in the atomic limit *do survive* upon adding a small $c>0$. This also implies that for very small c we expect the phase boundaries to be close to the ones at $c=0$ (i.e., to belong to the $d=0$ atomic phase diagram, Fig. 2). In practice there are of course some limitations. The perturbation in c can be used, strictly, only in the MI phase. In the MG phase perturbation in c cannot strictly apply, as the effect of c on ϕ_0 is of order c/α and thus generate terms as c^2/α in the energy, which dominate over c for small α. Thus as soon as the Hessian eigenvalues extend to 0 perturbation theory fails. In the MG phase this just means that due to possible multiple minima the ground state cannot be determined perturbatively. However, this only concerns the precise position of ϕ_n^0 in the well, but does not have any consequence on the fact that all ϕ_n^0 remain in a single well. These effects, which go beyond perturbation theory, will change the precise dependence of the boundaries as a function of c from a naive perturbative estimate, but we believe that the boundaries are *continuous* as $c\to 0$. The $d=0$ phase diagram should thus also approximately give the $d=1$ diagram for small c.

A useful approximation, used in Sec. III C to study the MG/AG transition, and which consists of replacing the interaction term by a mass $\frac{1}{2}m^2\phi^2$, can be checked in the atomic limit. It correctly gives the multicritical point at $v=m^2$, since it has a transition for $W=m^2$ (for $W<m^2$ there is a unique minimum with probability 1, while for $W>m^2$ there is a finite probability that there is a second minimum). By construction this approximate model cannot distinguish between the MG and AG phases, and is only used to describe the MI/MG transition.

One must emphasize that none of the transitions in the $d=0$ model in Fig. 2 survives if the local distribution of disorder is Gaussian. Indeed, the probability of a second minimum is always nonzero, although it can be exponentially small, resulting in a sharp crossover behavior rather than transitions. However, it is not so clear whether the same applies in higher dimensions. We know that the gap is robust to small bounded disorder. However for unbounded disorder, formation of terraces if size L become energetically favorable in rare regions with exponentially small probability. This leads to a gapless spectrum, with an exponentially (in $d>1$) small density of states at low energy. Note that although the gap itself can no longer be used as an order parameter, one can still clearly define a phase transition between MI and MG phases, since in the MG phase the spectrum is expected to become algebraic.

To conclude this section, we have established that for bounded disorder three phases (MI, MG, and AG) already exist in the atomic classical limit. Previous attempts at analyzing the classical limit[41] assumed that, beyond a length L_0, the distribution of the phase becomes random. As we find here, this is incorrect for weak disorder, and the phase instead has a narrow distribution around $\phi=0$. Thus these arguments missed the existence of the Mott glass phase, and the correlation length L_0 identified in Ref. 41 is not the correct one. In order to obtain more detailed information on the three phases when $d=1$ and higher we now turn to more sophisticated methods.

B. Replica variational method

Let us now use a Gaussian variational method[42,20] to study the action originating from Hamiltonian (12). In this section we only retain the backward scattering, which is the one leading to localization. The effect of forward scattering is analyzed in Appendix A. Let us recall that backward scattering is generated even if only commensurate and forward scatterings are present.

1. Derivation of the variational equations

Let us first briefly recall the principle of the method we use. The partition function of a disordered quantum system is

$$Z=\int d[\phi]e^{-S[\phi]/\hbar}, \tag{35}$$

where $S[\phi]$ is the Euclidean action that depends explicitly on the quenched disorder. In physical problems, one usually needs the average of the free energy

$$F=-\frac{1}{\beta}\overline{\ln Z}, \tag{36}$$

where the overbar denotes a disorder average. This average can be done via a replica trick:[43]

$$\ln Z = \lim_{n\to 0} \frac{Z^n - 1}{n}. \tag{37}$$

One has, for integer n,

$$\overline{Z^n} = \int \overline{\prod_{a=1}^{n} d[\phi_a] e^{-S_a[\phi_a]/\hbar}} = \int \prod_{a=1}^{n} d[\phi_a] e^{-S_{\text{rep.}}[\phi_a]/\hbar}, \tag{38}$$

where $S_{\text{rep.}}$ is a disorder-free quantity that depends on the n fields ϕ_a. In the end, one has traded the disorder average to a analytical continuation from an integer number of fields n to $n=0$. In our particular case, after having averaged over disorder action (8) leads to the replicated action

$$\begin{aligned}\frac{S_{\text{rep.}}}{\hbar} = \sum_a \Bigg[& \int \frac{dx d\tau}{2\pi K} \left(v(\partial_x \phi_a)^2 + \frac{(\partial_\tau \phi_a)^2}{v} \right) \\ & - \frac{g}{\pi\alpha\hbar} \int dx d\tau \cos 2\phi_a \Bigg] \\ & - \frac{W}{(2\pi\alpha\hbar)^2} \sum_{a,b} \int dx \int_0^\beta d\tau \int_0^\beta d\tau' \cos\{2[\phi_a(x,\tau) \\ & - \phi_b(x,\tau')]\},\end{aligned} \tag{39}$$

in which one has to take the limit $n\to 0$. One way to perform this limit is to use a Gaussian variational method (GVM) initially introduced to study classical disordered systems such as random heteropolymers,[44] random manifolds,[42] and vortex lattices.[40,20] This ansatz has been extended to treat correlated disorder, and thus to apply to quantum systems as well.[20] Since this method has been shown to describe with a good accuracy both the pure commensurate phase and the Anderson insulator phase on can also expect to obtain good results in this more complicated situation.

The ansatz consists of finding the ''best'' quadratic action

$$S_0 = \frac{1}{2\beta\hbar} \sum_{\omega_n} \int \frac{dq}{2\pi} \phi_a(q,\omega_n) G_{ab}^{-1}(q,\omega_n) \phi_b(q,\omega_n), \tag{40}$$

with

$$v G_{ab}^{-1}(q,\omega) = \frac{((vq)^2+\omega^2)}{\pi K} \delta_{ab} - \sigma_{ab}(q,\omega), \tag{41}$$

i.e., the one that minimizes the trial free energy:

$$F_{\text{var}} = F_0 + \frac{1}{\beta\hbar} \langle S_{\text{rep.}} - S_0 \rangle_{S_0} \tag{42}$$

$\langle \cdots \rangle_{S_0}$ designates the averages performed with respect to the Gaussian action, and F_0 is the free energy associated with Eq. (40), i.e.,

$$F_0 = \int \frac{dq}{2\pi} \frac{1}{\beta} \sum_n (\ln G)_{aa}(q,\omega_n). \tag{43}$$

In this method the full Green's functions $G(q,\omega)$ are the variational parameters. A derivation of the saddle-point equations is performed in Appendix B. Introducing $G_c(q,\omega_n) = \Sigma_b G_{ab}(q,\omega_n)$ and $B_{ab}(x,\tau) = G_{aa}(x,\tau) - G_{ab}(x,\tau)$ and parametrizing these $n\times n$ hierarchical matrices using Parisi's ansatz [$G_{a\neq b} \to G(u)$, $G_{aa} \to \tilde{G}$, and similarly for any quantity; see Appendix B], we obtain the saddle-point equations (B6):

$$\begin{aligned} G_c^{-1}(q,\omega_n) = & \frac{\hbar}{\pi K} \left(v q^2 + \frac{\omega_n^2}{v} \right) \\ & + \frac{4g}{\pi\alpha} \exp[-2\hbar \tilde{G}(x=0,\tau=0)] \\ & + \frac{2W}{\hbar(\pi\alpha)^2} \int_0^{\beta\hbar} d\tau [1-\cos(\omega_n\tau)] \\ & \times \Bigg[\exp[-4\hbar \tilde{B}(x=0,\tau)] \\ & - \int_0^1 du \exp(-4\hbar B(u)) \Bigg], \end{aligned} \tag{44}$$

with

$$\sigma(q,\omega_n,u) = \frac{2Wv}{(\pi\alpha)^2} \beta \exp(-\hbar 4B(u)) \delta_{\omega_n,0}. \tag{45}$$

In the absence of the commensurate potential, Eq. (44) is known to lead to a one-step replica symmetry-broken solution describing an Anderson localized phase,[20] the replica-symmetric solution being unstable. On the other hand, in the absence of disorder the commensurate phase (i.e., the Mott insulator phase) is obviously replica symmetric. Therefore, we will search first for a replica symmetric solution that we expect to be associated with a Mott insulating phase in Sec. III B 2. Above a certain disorder this solution will become unstable, and one has to turn to replica-symmetry-broken solutions. As we will see in Sec. III B 3, in the presence of a commensurate term, besides the saddle-point solution corresponding to the Anderson insulator phase there is room for a third saddle-point solution corresponding to the Mott glass phase.

2. Gapped replica-symmetric solution: Mott Insulator

For the replica-symmetric solution, $G(q,\omega_n,u) = G(q,\omega_n)$. The saddle-point equations then read

$$v G_c^{-1}(q,\omega_n) = \frac{\hbar}{\pi K} [(vq)^2 + \omega_n^2] + m^2 + I(\omega_n), \tag{46}$$

$$G(q,\omega_n,u) = \frac{2W\beta K^2}{(\hbar\alpha)^2} \frac{e^{-4\hbar G_c(0)} \delta_{\omega_n,0}}{[(vq)^2 + \pi\bar{K} m^2]^2}, \tag{47}$$

$$m^2 = \frac{4gv}{\pi\alpha} e^{-2\hbar\tilde{G}(0,0)}, \tag{48}$$

$$I(\omega_n)=\frac{2Wv}{(\pi\alpha)^2\hbar}e^{-4\hbar G_c(0,0)}\int_0^{\beta\hbar}d\tau(e^{4\hbar G_c(0,\tau)}-1)\times[1-\cos(\omega_n\tau)]. \tag{49}$$

In the general case, Eqs. (46)–(49) can only be solved numerically. However, in the limits $\hbar\to 0$ and $K\to 0$, $\bar{K}=K/\hbar$ fixed, it is possible to solve these equations analytically. This is due to the fact that in that limit m^2 has no dependence on $I(\omega_n)$, so that m is given by the simple equation

$$m^2=\frac{4gv}{\pi\alpha}\exp\left[-\frac{W\bar{K}^{1/2}}{\alpha^2\pi^{3/2}v^{1/2}m^3}\right]. \tag{50}$$

Self-consistent equation (50) always has the trivial solution $m=0$. Let us determine under which conditions it can also have a nontrivial solution with $m\neq 0$. In order to obtain the answer in physical terms, it is convenient to reexpress all quantities as a function of the physical lengths l_0 and d:

$$\frac{1}{l_0^3}=\frac{16W\bar{K}^2}{(\alpha v)^2}, \tag{51}$$

$$\frac{1}{d^2}=\frac{4g\bar{K}}{(\alpha v)}. \tag{52}$$

These correspond, respectively, to the localization (pinning) length in the absence of commensurability, and to the soliton size of the pure gap phase. We introduce the length

$$\xi^2=\frac{v^2}{(\pi\bar{K}m^2)}, \tag{53}$$

which, as we will see, is the correlation length in the presence of both the commensurate potential and the disorder. One can then rewrite Eq. (50) as:

$$\frac{1}{\xi^2}=\frac{1}{d^2}\exp\left[-\frac{1}{16}\left(\frac{\xi}{l_0}\right)^3\right]. \tag{54}$$

For $l_0/d>\frac{1}{2}(3e/4)^{1/3}$, this equation admits two solutions. It can be seen, by considering the limit of large disorder, that solutions with $l_0/\xi<\frac{1}{2}(\frac{3}{4})^{1/3}$ are spurious. Thus, for $l_0/d>\frac{1}{2}(3e/4)^{1/3}$, we have a unique solution of Eq. (54). For $l_0/d<\frac{1}{2}(3e/4)^{1/3}$, there is no solution, which means that the replica-symmetric solution with a mass is unstable. Since it is known[20] that a replica symmetric phase with no mass is unphysical for $\hbar\to 0$, this means that, for large enough disorder, we obtain a breaking of replica symmetry.

Let us now examine the equation for $I(\omega_n)$. An expansion around $\hbar=0$ in Eq. (49) gives the self-consistent equation for $I(\omega_n)$:

$$I(\omega_n)=\frac{8Wv}{(\pi\alpha)^2}\int_0^{\beta\hbar}G_c(x=0,\tau)[1-\cos(\omega_n\tau)]d\tau. \tag{55}$$

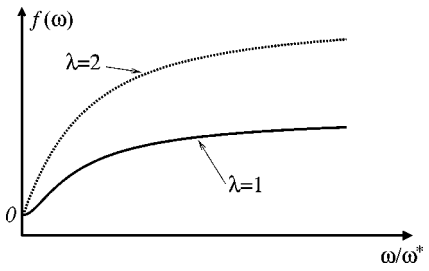

FIG. 7. The function f as a function of ω for $\lambda=1$ (full curve) and 2 (dashed curve). Note that as $\lambda=2$, f starts linearly with frequency, contrary to $\lambda<2$, for which f is quadratic at small ω.

Going to Fourier space and performing a q integration leads to to the final form

$$I(\omega_n)=\frac{4Wv\bar{K}}{\pi\alpha^2}\left[\frac{1}{\sqrt{\pi\bar{K}m}}-\frac{1}{\sqrt{\omega_n^2+\pi\bar{K}[m^2+I(\omega_n)]}}\right]. \tag{56}$$

Obviously,

$$I(\omega_n)=m^2 f\left(\frac{\omega_n}{\sqrt{\pi\bar{K}m}}\right), \tag{57}$$

where f satisfies the equations

$$f(x)=\lambda\left[1-\frac{1}{\sqrt{1+x^2+f(x)}}\right] \tag{58}$$

and

$$\lambda=\frac{4W\bar{K}^{1/2}v}{\pi^{3/2}\alpha^2m^3}=\frac{1}{4}\left(\frac{\xi}{l_0}\right)^3. \tag{59}$$

As can be seen from Eq. (46), m defines the correlation length ξ in the presence of *both* the commensurate and random potentials.

Once $m\neq 0$ is known from Eq. (50), λ and therefore f and $I(\omega_n)$ are entirely determined. The above equations thus completely fix all the parameters of the gapped replica-symmetric (RS) phase.

For $\lambda<2$, there is a physical solution of Eq. (58) such that $\lim_{x\to\pm\infty}f(x)=1+\lambda$ and for $x\ll 1$, $f(x)=1+\alpha x^2+o(x^2)$ with $\alpha=\lambda/(2-\lambda)$. The corresponding behavior of $f(x)$ as a function of ω is shown in Fig. 7 for $\lambda=1$. For $\lambda=2$, for $x\ll 1$, $f(x)=1+(2/\sqrt{3})|x|+O(x^2)$ and $\lim_{x\to\infty}f(x)=3$. The corresponding graph of $f(x)$ is also shown in Fig. 7. For $\lambda>2$ Eq. (58) has no physical solution. Thus, $\lambda=2$ is the boundary for the gapped RS phase. Putting $\lambda=2$ into Eq. (59) leads to $l_0/\xi=\frac{1}{2}>\frac{1}{2}(\frac{3}{4})^{1/3}$. Reinjecting this value into Eq. (54) gives

$$\frac{l_0}{d}=\frac{1}{2}e^{1/4}. \tag{60}$$

This point is in the domain where Eq. (54) still has solutions. Therefore, as disorder increases the system attains the point

where $\lambda=2$ *before* reaching the point where $m=0$. Beyond the point $\lambda=2$ the replica-symmetric solution becomes unstable. This leads us to consider a replica-symmetry-breaking solution of Eq. (44) for $l_0/d<e^{1/4}/2$, allowing for a nonzero m. The corresponding phase will thus not be the simple Anderson-localized phase expected from the strong-coupling RG argument.[62]

3. Replica-symmetry-broken solution

In Sec. III B 2, we have seen that in the limit $\hbar\to 0$ a replica-symmetric solution of Eqs. (44) can exist for $\lambda\leqslant 2$ but is unstable for $\lambda>2$. In this section, we consider in the limit $\hbar\to 0$ the one-step replica-symmetry-breaking (RSB) solution of Eqs. (44). Such a RSB solution should be valid for $\lambda>2$, and is known to correctly describe the simple Anderson insulating phase for the simple disordered case.[20] Compared to the case in the absence of commensurate potential, we have to allow, in our RSB solution, for $m^2\neq 0$. However, contrary to the RS case, a RSB solution with $m^2=0$ is perfectly possible,[20] and corresponds to the case in which the commensurate potential is completely washed out by the random potential.

Two scenarios could thus be *a priori* possible. Either one obtains a RSB solution with $m^2=0$ similar to the solution of Ref. 20 as soon as the replica-symmetric solution becomes unstable, or there exists an intermediate regime with both a RSB selection and $m^2\neq 0$. The first case would correspond to the simple scenario, suggested from extrapolating the RG of a direct transition between the commensurate phase and the Anderson insulator. On the other hand the behavior in the RS solution strongly suggests the existence of an intermediate phase: the Mott glass phase. Indeed in the RS phase the optical gap closes, leading to a conductivity very similar to the simple Anderson conductivity, whereas the compressibility remains zero. This suggests that all effects of the commensurate potential have not yet disappeared, and that the system is not in a simple Anderson regime. As we will see, this is the second possibility that is obtained, leading thus to a much richer physical behavior than could have been guessed from the RG extrapolations.

The saddle point equations (44) are first rewritten as

$$v G_c^{-1}(q,\omega_n)=\frac{1}{\pi K}[(vq)^2+\omega_n^2]+m^2 + \Sigma_1(1-\delta_{n,0})+I(\omega_n), \tag{61}$$

$$I(\omega_n)=\frac{2Wv}{(\pi\alpha)^2\hbar}\int_0^{\beta\hbar}[e^{-4\hbar\tilde{B}(\tau)}-e^{-4\hbar B(u>u_c)}] \times[1-\cos(\omega_n\tau)]d\tau, \tag{62}$$

$$\Sigma_1=u_c[\sigma(u>u_c)-\sigma(u<u_c)]=[\sigma](u>u_c), \tag{63}$$

$$\sigma(u)=\frac{2Wv}{(\pi\alpha)^2}e^{-\hbar 4B(u)}\beta\delta_{n,0}, \tag{64}$$

$$m^2=\frac{4gv}{\pi\alpha}e^{-4\hbar\tilde{G}(0)}, \tag{65}$$

where we look for a one step RSB solution, as is adapted to $d=1+1$. The parameters m, Σ_1 and the breakpoint u_c have to be determined self-consistently. The full solution is given in Appendix C. The parameter u_c is determined from the marginality of the replicon condition, which has been shown[20] to be the correct condition to impose. This leads to $I(\omega_n)\propto|\omega_n|$. One can check (see Appendix C and Sec. III B 2) that this condition is also satisfied by $I(\omega_n)$ at the limit of stability of the RS solution. The two other parameters m and Σ_1 depend on the ratio d/l_0.

As is shown in Appendix C for $d/l_0>1.86$, one has $m=0$ and $\Sigma_1\neq 0$. This solution is thus similar to the one of a disordered system without the commensurate potential, and corresponds to an Anderson glass (insulator). Such a phase has no gap in the optical conductivity.[20] Since there is no mass in propagator (61) for $\omega_n=0$, the compressibility is finite.

On the other hand for $d/l_0<1.86$ the solution has a finite mass. This regime is thus different from the simple Anderson insulator. The physical properties (conductivity, phason density of states, compressibility) will be discussed at length in Sec. IV. An important result of Sec. IV is that because of the presence of the mass the system is still incompressible while having the conductivity of an Anderson insulator phase. This is the Mott glass phase,[25] which shares some properties of the Mott insulator (incompressibility) phase with those of a glassy phase (breaking of replica symmetry).

Therefore, the physical picture is the following: for $d/l_0<2e^{-1/4}$, one has a replica-symmetric solution with a gap in the conductivity, the Mott insulator phase; for $2e^{-1/4}<d/l_0<1.86$, one has a RSB solution without a gap in the conductivity but zero compressibility, the Mott Glass phase; and finally, for $d/l_0>1.86$, there is a finite compressibility and no gap in the conductivity, the anderson insulator phase. In other words, one recovers the solution of Ref. 20 not as soon as $d/l_0>2e^{-1/4}$, as we would expect from extrapolations of the perturbative $d=1$ renormalization-group calculations, but only at the higher value $d/l_0>1.86$. This is due to the formation of an intermediate phase, which is both incompressible but without a gap in the conductivity. This intermediate phase being an intermediate coupling one, the failure of the perturbative renormalization-group approach to predict its existence is not a surprise. In a forthcoming section, we will discuss its properties in detail. The phase diagram as a function of d/l_0 is represented in Fig. 8. Let us remark that all transitions appear to be first order within the GVM formalism.

C. Mott insulator to Mott glass transition: Functional renormalization-group study and classical equivalent

In this section we study phase model (15) in an arbitrary dimension d using a renormalization-group method perturbatively controlled in $d=4-\epsilon$ and small $\hbar$. This provides useful information on interacting fermions with disorder by continuation down to $d=1$ (as we do not expect drastic changes

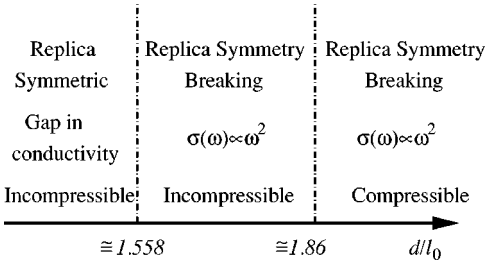

FIG. 8. The phase diagram of a commensurate system with backward scattering only as a function of d/l_0 (disorder increases when d/l_0 increases). At weak disorder, $d/l_0 \ll 1$, one obtains an incompressible phase with a gap in the conductivity i.e., a Mott Insulator. For strong disorder, $d/l_0 \gg 1$, one has a compressible phase with a conductivity that behaves as $\sigma(\omega) \propto \omega^2$, i.e., an Anderson glass. The surprising feature of this phase diagram is the appearance of an intermediate incompressible phase (like the Mott insulator) having the same conductivity as an Anderson glass for $d/l_0 \sim 1$.

in this model down to $d=1$ for small $\hbar$). We will perform the analysis in the notations of the classical equivalent model, but also give some conclusions in terms of the parameters of the quantum model, via relations (23).

As is well known for classical problems such as manifolds in random media,[45–47] the functional renormalization group (FRG) method provides an alternative to the Gaussian variational method. The FRG method accurately treats the nonlinearities, and does not use replica symmetry breaking. When the two methods are supposed to be exact and are compared, they do agree, as found for the random manifold problem[48] for $N \to \infty$, and generally give consistent physics.[40] Here we will use the FRG method as a check of the correctness of the prediction by the GVM of the Mott glass phase, and as a way to obtain additional detailed information on the Mott insulator to Mott glass phase transition (see Fig. 9).

Although this is not the route we follow here one can apply the FRG method directly to the model of Eqs. (15)–(22). This amounts to generalizing to correlated disorder the study of Refs. 49–51 made for the case of uncorrelated disorder. This shows that a commensurate potential becomes

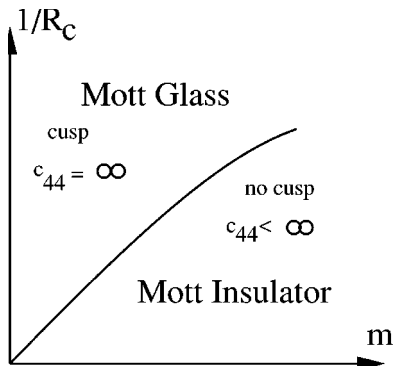

FIG. 9. Phase diagram of the effective model from the FRG phase, at $T=0$ ($\hbar=0$). $R_c \sim (1/W)^{1/(4-d)}$ is the Larkin length (localization length), and parametrizes disorder strength. These phases and transition survive at $T>0$ ($\hbar>0$).

relevant, and may lead to a description of the transition between a gapless Anderson glass phase to a gapped phase. But this route would not give us the information we want about the nature of the gapped phase, i.e., it cannot distinguish between the Mott glass and Mott insulator phase. Indeed, the approach of Refs. 49–51 fails to describe the phase where the commensurate potential is relevant since the FRG method then flows to strong coupling.

Thus, in order to test for the existence of a Mott glass phase, we consider from the start a situation where the commensurate potential is relevant and replace the full model [Eqs. (15)–(22)] by an effective model in which the sine Gordon term is replaced by a quadratic mass term:

$$V_p(\phi) \to \frac{m^2}{2}\phi^2. \tag{66}$$

This should be a reasonable approximation when the sine Gordon term is relevant, and is in the spirit of the self-consistent harmonic approximation. Our approximation amounts to neglecting some soliton excitations by giving them large energy, and to neglecting the renormalization of the gap by disorder. This simplified model has the merit of being amenable to a *perturbatively* controlled study in $d=4-\epsilon$. We will show that it does exhibit a phase transition at $T_{cl}=0$ ($\hbar=0$) which survives at $T_{cl}>0$ ($\hbar>0$), and can be identified with the Mott insulator to Mott glass phase transition. This model thus allows us to study the formation of the Mott glass phase.

We have obtained the FRG equations for the effective model [Eq. (66)]. They can be derived by integrating out iteratively short wavelength modes, extending.[46,47,52–54] They are obtained in terms of the running dimensionless disorder $\tilde{\Delta}(\phi,l) = -\tilde{R}''(\phi,l)$, the running dimensionless temperature $\tilde{T}_l \sim T$, both defined in Appendix D, and the tilt modulus $c_{44}(l)$. These RG equations read

$$\partial_l \tilde{\Delta}(\phi) = \epsilon\tilde{\Delta}(\phi) + \tilde{T}_l\tilde{\Delta}''(\phi) - f(l)\{\tilde{\Delta}''(\phi)[\tilde{\Delta}(0)-\tilde{\Delta}(\phi)] - \tilde{\Delta}'(\phi)^2\}, \tag{67}$$

$$\partial_l c_{44} = -f(l)\tilde{\Delta}''(0)c_{44} \tag{68}$$

with $\epsilon = 4-d$, setting $c=1$ (as c is not renormalized),

$$f(l) = \frac{1}{(1+\mu e^{2l})^2} \tag{69}$$

comes from the integration of the high momentum modes. Here $\mu = (m\alpha)^2$. These FRG equations are analyzed in Appendix D. Here we describe only the main results.

At $T=0$ (i.e., $\hbar \to 0$ for the quantum problem) we find that there is a phase transition. One can measure the strength of the bare disorder using the Larkin length $R_c \sim [1/\tilde{\Delta}''_{l=0}(\phi=0)]^{1/(4-d)}$ of the problem without commensurate potential (corresponding to the localization length for the $d=1$ fermion problem). Then we find that, for a given m, there is a transition at a critical disorder strength

$$R_c \equiv \left(\frac{1}{\tilde{\Delta}''_{l=0}(\phi=0)} \right)^{1/(4-d)} = C\frac{1}{m}, \tag{70}$$

where C is a constant. The two phases are the following: (i) For strong disorder $R_c < C(1/m)$, we find that $\Delta_2(l) = -\tilde{\Delta}''(0,l)$, the fourth derivative of the renormalized disorder correlator $R_l(u)$, becomes infinite at a finite scale $R_c^*(m)$, i.e., the disorder correlator becomes nonanalytic and develops a cusp singularity at a scale $R_c^*(m)$. For the problem in the absence of a mass the cusp generation at the Larkin length $R_c^*(m=0) = R_c$ is well known to be associated with the existence of many metastable states beyond R_c. This cusp generation is associated with the apparition of the transverse Meissner effect in vortex lattices pinned by columnar disorder[52] (and to the appearance of RSB in the GVM treatment[20]). As will be discussed below, this phase corresponds to the *Mott glass* phase, (ii) For weak disorder $R_c > C(1/m)$, the flow is cut by the presence of the mass before a cusp can be generated. This phase does not exhibit metastable states and corresponds to the *Mott insulator* phase.

Since the mass can be chosen arbitrarily small, the study is thus perturbative in disorder in $d = 4 - \epsilon$ for model (66). It is interesting to note that this $T=0$ transition exists both for correlated and uncorrelated disorders. However, this transition is stable to finite temperature only for correlated disorder. Indeed, for pointlike disorder the temperature rounds the cusp,[55,56] which implies that there can exist no sharp distinction between the two phases at finite temperature. In addition, the quadratic part of the Hamiltonian is not renormalized by disorder, and thus even at $T=0$ there cannot be any signature of the transition on two-point correlation functions of ϕ. Thus it is possible that the transition observed in Ref. 57 is an artifact of the method used. On the contrary, for correlated disorder, there is a genuine transition, and (because of the lack of rotational invariance [in (x,τ)], the existence of a cusp, and the transition directly affects for correlated disorder), two-point correlation functions.

The FRG approach gives immediate information on the renormalized tilt modulus [see Eq. (23)] $c_{44}^R = c_{44}(+\infty)$. Since this is also the coefficient of ω^2 in the Green function $\langle \phi\phi \rangle$, one can infer from it that if c_{44} is finite the Green function is likely to remain analytic, and thus *that there is a gap in the conductivity*. If c_{44} becomes infinite then the Green function is not analytic and no gap should exist in the conductivity. The FRG approach gives that

$$\frac{c_{44}(+\infty)}{c_{44}(0)} = \frac{\left(\frac{R_c}{a}\right)^{\epsilon} - 1}{\left(\frac{R_c}{a}\right)^{\epsilon} - \left(\frac{R_c^*(\mu)}{a}\right)^{\epsilon}}, \tag{71}$$

and thus we find that phase (i) above, which corresponds to a cusp ($c_{44}^R = +\infty$), can be identified with a Mott glass phase while phase (ii) above, which corresponds to no cusp ($c_{44}^R < +\infty$), can be identified with a Mott insulator phase. The gap itself can be estimated as

$$\Delta = m/\sqrt{c_{44}^R} \sim \left(R_c - \frac{C}{m} \right); \tag{72}$$

thus it vanishes linearly $\Delta \sim [R_c - (C/m)]$ at the MI to MG phase transition. Correlation functions are also estimated in Appendix D.

One of the most crucial test is to show that the above MI-MG phase transition survives to quantum fluctuations $\hbar > 0$ (thermal fluctuations $T>0$ for the $d+1$ classical model). This is the case, and the calculation is detailed in Appendix D. There is no doubt that the MI phase survives to quantum fluctuations; however, it is less obvious that the MG phase would survive. Indeed, the cusp is rounded by the effective temperature variable $\tilde{T}_l \sim T/\sqrt{c_{44}(l)}$. However, the key point is that $c_{44}(l)$ becomes very large as soon as the second derivative Δ_2 grows, and as a consequence the effective temperature $\tilde{T}$ renormalizes to exactly zero *at a finite scale* (as it does in the absence of a mass). Thus the Mott glass phase survives at a finite temperature. A similar phenomenon was also found recently in the dynamics of classical periodic systems with correlated disorder.[53]

To conclude this section, the FRG approach shows, within a $d = 4 - \epsilon$ analysis of the effective model with mass, that a transition exists at large K in the quantum problem (and at low temperature in the equivalent classical problem) between a MI phase at weak disorder with analytic Green function, no metastable states and a gap in the conductivity and a Mott Glass phase with metastable states, no gap in the conductivity at stronger disorder. This allows one to predict that the conductivity gap should close linearly at the transition (at least in the limit of small $K \to 0$).

IV. PHYSICAL PROPERTIES, RESULTS IN $d=1$, AND EXTENSIONS TO HIGHER DIMENSIONS

A. $d=1$

1. Compressibility, density of states, and correlation functions

In this section, we define and calculate equilibrium thermodynamic quantities such as the compressibility or the phason density of states of the system. One of the most striking differences between the Anderson insulator (AI) and (MI) phases is that the former is compressible whereas the latter is incompressible. The compressibility is given, in any dimension, by

$$\chi(q,\omega_n) = \frac{1}{\hbar} \int d^d x \int_0^{\beta\hbar} d\tau e^{-i(qx - \omega_n \tau)} \times \overline{\langle T_\tau [n(x,\tau) - \langle n(x,\tau) \rangle][n(0,0) - \langle n(0,0) \rangle] \rangle}, \tag{73}$$

where n is the density. This leads to the average static compressibility $\chi_s = \lim_{q\to 0}[\lim_{\omega \to 0} \chi(q,\omega)]$. In $d=1$, using the bosonic expression for the density [Eq. (73)] leads to

$$\chi_s = \lim_{q\to 0} \lim_{\omega \to 0} q^2 G_c(q,\omega), \tag{74}$$

where

$$G_c(q,\omega)=\overline{\langle\phi_{q,\omega}\phi_{-q,-\omega}\rangle-\langle\phi_{q,\omega}\rangle\langle\phi_{-q,-\omega}\rangle}. \quad (75)$$

Another thermodynamic quantity of interest is the phason density of states:

$$\rho(\omega)=-\frac{\hbar}{\pi v}\mathrm{Im}[i\omega_n\tilde{G}(x,x,i\omega_n)]|_{i\omega_n\to\omega+i0_+}. \quad (76)$$

In the $\overline{K}\to 0$ limit, Eq. (76) describes the phason density of states of a classical charge-density wave pinned by *both* the commensurate and random potentials.[41,58] Using Eq. (46), one obtains the following expression for the density of states ρ:

$$\rho(\omega)=-\frac{K}{2}\mathrm{Im}\left[\frac{i\omega_n}{\sqrt{\omega_n^2+\pi\overline{K}(m^2+I(\omega_n))}}\right]_{i\omega_n\to\omega+i0_+} \quad (77)$$

Various correlation functions can also be computed. In particular the on-site (CDW) and bond (BOW) charge density. For spinless fermions these read

$$\chi_{CDW}=\langle(c_i^\dagger c_i)(c_j^\dagger c_j)\rangle, \quad (78)$$

$$\chi_{BOW}=\langle(c_{i+1}^\dagger c_i+\text{H.c.})(c_{j+1}^\dagger c_j+\text{H.c.})\rangle. \quad (79)$$

In the boson representation the $2k_F$ part of these correlation function are related to the $\cos(2\phi)$ and $\sin(2\phi)$ correlation functions:

$$\chi_{CDW}\propto(-1)^x\overline{\langle\cos[2\phi(x)]\cos[2\phi(0)]\rangle}=K_\parallel(x), \quad (80)$$

$$\chi_{BOW}\propto(-1)^x\overline{\langle\sin[2\phi(x)]\sin[2\phi(0)]\rangle}=K_\perp(x). \quad (81)$$

Let us now compute these various quantities using the results of the variational method presented in Sec. III B for each of the three phases.

(a) *Mott insulator phase*. This corresponds to the RS phase obtained at weak disorder ($d/l_0<2e^{-1/4}$). Because of the nonzero m the whole MI phase is thus incompressible [see Eq. (46)]. The MI phase is thus the direct continuation of the nondisordered commensurate phase. In the MI phase, the disorder is too weak to be able to overcome the gap.

In the replica-symmetric case, $\rho(\omega)$ can be expressed in terms of the function f defined by Eq. (58) in the form

$$\rho(\omega)=-\frac{K}{2}\mathrm{Im}\left(\frac{x}{\sqrt{1+f(-ix)-x^2}}\right)=\frac{K}{2\lambda}x\,\mathrm{Im}\,f(-ix). \quad (82)$$

Where $x=\omega/\omega^*$ and $\omega^*=v/\xi$. To perform the analytical continuation in Eq. (82), we transform Eq. (58) into a cubic equation for f with coefficients depending on x^2 and λ. Although this transformation adds two spurious solutions that do not satisfy $f(0)=0$, it proves extremely useful, as performing an analytical continuation amounts to solving the cubic equation for f with $x^2\to -x^2$. Equation (82) implies that the phason density of states in nonzero only when f has a nonzero imaginary part. For $\lambda<2$, $f(-ix)$ is real for

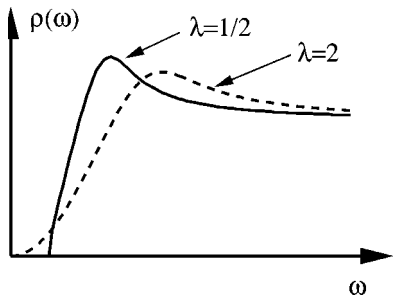

FIG. 10. The behavior of the density of states as a function of ω for $\lambda=1/2$, 1, and 2. For $\lambda=1$, and 1/2, there is a gap in the density of states for $\omega<\omega_c(\lambda)$. ω_c decreases with increasing λ. For $\lambda=2$, the gap disappears, and the density of states behaves as $\rho(\omega)\sim\omega^2$, i.e., there is a pseudogap. The pseudogap persists in the whole RSB phase. Note that the maximum in the density of states decreases as ω increases, indicating a transfer of spectral weight to low frequencies.

$$x<x_c=\sqrt{1+\lambda-3\left(\frac{\lambda}{2}\right)^{2/3}}. \quad (83)$$

As a consequence, in the MI phase, there is a gap in the phason density of states for $\omega<\omega_c=\omega^*x_c$:

$$\rho(\omega)=0, \quad \omega<\omega_c. \quad (84)$$

The physical interpretation of such a form for the density of states is obvious: no states are available below the gap. Thus, in the Gaussian variational framework, there are no discrete two particle states (i.e., excitons) below the gap. For $\omega\to\omega_c+0$ we obtain $\rho(\omega)\sim(\omega-\omega_c)^{1/2}$. At high frequencies, we obtain $\rho(\omega)\to K/2$, i.e., the density of state goes to a constant. A plot of $\rho(\omega)$ is shown in Fig. 10.

In the replica framework, we have the following general expressions for $K_\parallel$ and $K_\perp$ [see Eqs. (A12) and (A13)]:

$$K_\parallel=e^{-\hbar 2\tilde{G}(0)}\cosh[\hbar 2\tilde{G}(x)], \quad (85)$$

$$K_\perp=e^{-\hbar 2\tilde{G}(0)}\sinh[\hbar 2\tilde{G}(x)]. \quad (86)$$

In the replica-symmetric case, for $\hbar\to 0$ and $\overline{K}=K/\hbar$ fixed, one finds

$$\hbar\tilde{G}(x)=\frac{\xi^3}{32l_0^3}\left(1+\frac{|x|}{\xi}\right)e^{-|x|/\xi}. \quad (87)$$

The resulting correlation functions are

$$K_\parallel(x)=e^{-\xi^3/16l_0^3}\cosh\left[\frac{\xi^3}{16l_0^3}\left(1+\frac{|x|}{\xi}\right)e^{-|x|/\xi}\right], \quad (88)$$

$$K_\perp(x)=e^{-\xi^3/16l_0^3}\sinh\left[\frac{\xi^3}{16l_0^3}\left(1+\frac{|x|}{\xi}\right)e^{-|x|/\xi}\right]. \quad (89)$$

For $x\to\infty$, one has $K_\parallel(x)\to e^{-\xi^3/16l_0^3}$. This implies that $\langle\cos 2\phi\rangle=d/\xi$. Therefore, in the Mott insulator phase, charge-density-wave order is still present, but the order is reduced with respect to the pure system in which one would

have $\langle \cos 2\phi \rangle = 1$. Even for $x \to 0$, the CDW order of the pure system is not recovered. Another interesting property is that some BOW order is also induced at short distances, although BOW order is not present at long distance. The presence of BOW order is due to the random phase in ϕ induced by disorder. When the random phase is of order $\pi/2$, this implies local BOW order. However, the positions at which BOW order is obtained are not correlated with each other in the system. This explains the exponential decay of BOW order.

(b) Anderson glass and Mott glass phase. For $d/l_0 > 1.86$ the system is in the AG phase. In this phase, using Eq. (74) and the expression for G_c, one finds that the compressibility is identical to the one of the pure system $\chi_s = \overline{K}/\pi^2 u$. Such a result is due to the fact that the Gaussian variational method does not take into account the renormalization of K by disorder. Nevertheless, the replica variational approximation correctly gives a nonzero compressibility for an Anderson glass. We stress that these results are valid independently of the presence and absence[20] of the commensurate potential.

In the intermediate MG phase, with both RSB and a gap that is obtained for $2e^{-1/4} < d/l_0 < 1.86$, $m \neq 0$, we obtain a zero compressibility. One would therefore be tempted to associate this phase with a Mott insulator. However, the forthcoming calculation of the conductivity in Sec. IV A 2 will show that this intermediate phase is *not* a Mott Insulator.

In the replica-symmetry-breaking case, formulas (77) and (82) remain valid. However, the function f that must be used in Eq. (82) corresponds to $\lambda = 2$ in Eq. (58). This means that as long as there is a RSB solution of the variational equations, there is a pseudogap in the phason density of states. The behavior of the density of states as a function of ω is represented in Fig. 10.

In the case with broken replica symmetry, one has

$$K_{\parallel}(x) = e^{-2\hbar\langle G(0)\rangle} \cosh[2\hbar\langle G(x)\rangle], \tag{90}$$

$$K_{\perp}(x) = e^{-2\hbar\langle G(0)\rangle} \sinh[2\hbar\langle G(x)\rangle], \tag{91}$$

where we have taken into account the fact that as $\hbar \to 0$, $\hbar G_c(x) \to 0$, and $\langle G(x)\rangle = \int_0^1 du G(x,u)$. Using one-step expressions, we obtain

$$\hbar\langle G(x)\rangle = \frac{e^{\varphi}}{\mu^3(\varphi)}\left[\left(1 + \frac{\mu|x|}{2l_0}\right)e^{-\mu|x|/(2l_0)}\right] + \frac{1-e^{\varphi}}{2(1-\mu^2(\varphi))}\left[\frac{e^{-\mu|x|/2l_0}}{\mu} - e^{-|x|/(2l_0)}\right]. \tag{92}$$

We see that in the Mott glass phase the CDW order is still present, in analogy with the Mott insulator phase. Such a behavior is in agreement with the predictions from the atomic limit of Sec. III A. This time, $\langle \cos 2\phi \rangle = \exp\{-e^{\phi}/[2\mu^3(\phi)]\}$. When the system becomes an Anderson insulator phase, $\langle \cos 2\phi \rangle = 0$, which seems to indicate a first-order transition. Such a first-order transition is likely to be only an artifact of the variational approach. Some subdominant BOW correlations are also present in the system. They decay exponentially with x, and since $\mu(\phi) < 1$, the correlation length of BOW and CDW fluctuations is $2l_0/\mu(\varphi)$. It is interesting to note that at the Mott insulator–Mott glass phase transition, the correlation length is continuous. However, there could be a slope discontinuity which would be characteristic of a second order phase transition.

2. Transport properties

To differentiate between Mott and Anderson glass phases, a crucial physical quantity is the ac conductivity. In the Mott insulator phase, the ac conductivity is zero for frequencies smaller than the gap whereas in the Anderson glass phase the ac conductivity behaves as $\sigma(\omega) = \omega^2(\ln \omega)^2$ in one dimension.[35,34] Within the GVM, in order to compute the conductivity it is sufficient to know m, Σ_1, and the analytical continuation of $I(\omega_n)$ to real frequencies. Using the Kubo formula, it is straightforward to show[20] that

$$\sigma(\omega) = \frac{v\overline{K}}{\pi} \frac{-i\omega}{\pi\overline{K}[m^2 + I(-i\omega)] - \omega^2}, \tag{93}$$

where $I(i\omega)$ represents the analytical continuation of $I(\omega_n)$ to real frequencies. Introducing the function f, defined in Eq. (58), one has

$$\sigma(\omega) = \frac{v\overline{K}}{\pi\omega^*} \frac{ix}{(1 + f(-ix) - x^2)}, \tag{94}$$

where $x = \omega/\omega^*$. Similar to the density of states, the behavior of the conductivity is therefore controlled by $\lambda = \frac{1}{4}(\xi/l_0)^3$. One can explicitly check that Eq. (93) satisfies the sum rule

$$\int_0^{\infty} d\omega \sigma(\omega) = \frac{v\overline{K}}{\pi}. \tag{95}$$

(a) Mott insulator phase. Let us begin with the conductivity for $\lambda < 2$, i.e., in the Mott insulator phase. It is easily seen that in order to obtain a nonzero real part of the conductivity one must have $\Im f(ix) \neq 0$. As a consequence, the real part of the frequency dependent conductivity is zero for $\omega < \omega_c$ where ω_c is the threshold below which the two particle density of states is zero [see Eq. (84)]. Physically, this means that there are no available two-particle excitations to absorb energy if $\omega < \omega_c$ i.e., at energies below the Mott gap. For $x > x_c$ ($\omega > \omega_c$), the analytical continuation of f to imaginary x has a nonzero imaginary part that leads to a nonzero real part of the frequency dependent conductivity. For x close to the threshold,

$$\mathrm{Im}\, f(x) = \frac{2}{\sqrt{3}}\left(\frac{\lambda}{2}\right)^{1/3}\sqrt{x^2 - x_c^2}. \tag{96}$$

As a consequence, for $\omega > \omega_c$ and close to the threshold, the real part of the conductivity behaves as $\mathrm{Re}\,\sigma(\omega) \sim (\omega - \omega_c)^{1/2}$ i.e., it is controlled by the available two-particle density of states. At large frequency, it can be shown that $\mathrm{Re}\,\sigma(\omega) \sim \lambda/x^4$. This behavior can be recovered by a simple perturbative calculation in disorder strength. Obviously, the

FIG. 11. The real part of the frequency dependent conductivity in the MI phase for $\lambda=1$ as a function of frequency.

conductivity shows a maximum at a frequency $\omega_m = \omega^* x_m(\lambda)$. The typical behavior of the real part of the conductivity for $\lambda=1$ is represented in Fig. 11. The behavior of the threshold frequency ω_c a function of λ is represented in Fig. 12.

(b) Mott glass and Anderson glass phases. For $\lambda \to 2$ the gap goes to zero as $2-\lambda$. Quite remarkably, for $\lambda=2$, there is *no* gap in the real part of the conductivity although the system is *still* incompressible. The real part of the conductivity goes to zero as $\omega \to 0$ as $\mathrm{Re}\,\sigma(\omega) \sim \omega^2$. The behavior of the conductivity for $\lambda=2$ is represented in Fig. 13. As for $\lambda<2$ when $x \to \infty$, the real part of the conductivity decreases as λ/x^4. In fact, this form of the conductivity is the one that is obtained in the Anderson glass phase in the *absence* of any commensurate potential.[20] Moreover, in the GVM framework, the Anderson glass is a RSB phase.[20] It can be easily seen that for all $\lambda \geqslant 2$, i.e., in all the RSB phases, the scaled conductivity is equal to the one of the Anderson glass phase. The conductivity in the MG and AG phases is thus also the one shown in Fig. 13. This remarkable pinning of the scaled conductivity at $\lambda=2$ is a consequence of the marginality condition.

3. General phase diagram in d=1

We have thus generically identified three phases for a disordered commensurate system. The bosonization representation being quite general in $d=1$ this also applied to bosons or spin chains.

All the previous results having been obtained in the limit where K is small, an important question is the range of stability of these three phases. Although, in principle, the variational method could help answering this questions, we do not

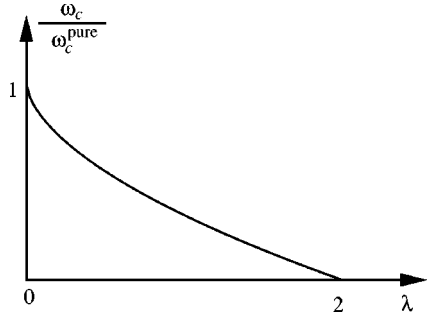

FIG. 12. The variation of the gap in the frequency-dependent conductivity as a function of λ. The gap in the conductivity goes to zero linearly for $\lambda \to 2$.

FIG. 13. The real part of the frequency-dependent conductivity in the MG and AG phases for $\lambda=2$ as a function of frequency. For small ω, $\sigma(\omega) \sim \omega^2$.

attempt this complicated calculation here, and instead give physical arguments.

It is clear that repulsive enough and finite range interactions are needed for the existence of a MG phase. A general argument is given in Sec. IV B. We note here that the case of infinite range (Coulomb) interaction is a (rather peculiar) example of a MG phase. Indeed, a one-dimensional Wigner crystal[31] has a compressibility

$$\chi_s = \lim_{q \to 0} \frac{q^2}{q^2 \log(1/q)} = 0;$$

nevertheless it has only a pseudogap in the conductivity[30,59] of $\sigma(\omega) \sim \omega^{\alpha}$. One can also show that, in a noninteracting system, the compressibility gap is equal to the gap for single-particle excitations. In particular, this means that the intermediate phase cannot exist for $K=1$. This result is in agreement with the self-consistent Born approximation calculation of Mori and Fukuyama[3] for the noninteracting case, which do not show any intermediate phase. Thus it can only exist for $K \leqslant K_c < 1$.

Let us now give a schematic phase phase diagram, which summarizes the effects of both backward and forward scattering in one dimension. As shown in this section forward scattering can also lead to gap closure. The phase diagram, as function of the Luttinger liquid parameter K and the strength of the forward D_f and backward D_b scattering is represented in Fig. 14.

B. General arguments and higher dimensions *d*>1

1. Interacting fermionic systems: excitonic argument

The physics leading to the MG phase is quite general, and persists in higher dimensions as well, as can be understood through a physical argument. Let us consider the atomic limit, where the hopping is zero. One can compute in this limit the gaps to create both single particle and particle-hole excitations (see Fig. 15) Let us consider for example fermions with spin with both an onsite repulsion U and a nearest-neighbor repulsion V, with one particle per site. Such a system is described by

$$H = U \sum_i n_{i\uparrow} n_{i\downarrow} + V \sum_{\langle i,j \rangle} n_i n_j + \sum_i W_i n_i - \mu \sum_i n_i , \tag{97}$$

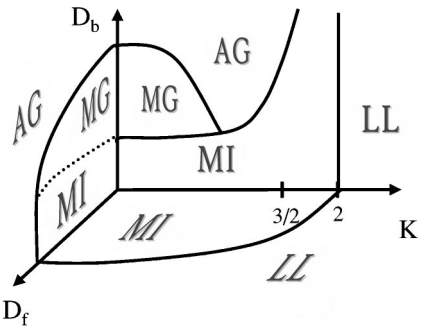

FIG. 14. Phase diagram of a one-dimensional system with both forward and backward scattering random potentials. The dashed lines correspond to phase boundaries between the Mott glass (MG) and the Mott Insulator (MI), the Anderson Insulator (AI) and the Luttinger liquid (LL) phases. The separation between the MG and MI phases in the presence of forward scattering disorder is drawn with question marks, since we do not know how forward scattering affects the competition of the MI of the MG phase.

where $n_i = n_{i\uparrow} + n_{i\downarrow}$, and W_i is the disorder potential. The energies to add E_{+1} or remove E_{-1} a particle at or from site i are

$$E_{+1,i} = E_{\rm gs} + U + zV - \mu + W_i, \tag{98}$$

$$E_{-1,i} = E_{\rm gs} - zV + \mu - W_i, \tag{99}$$

and $E_{\rm gs}$ is the energy of the ground state of the system with one particle per site. If one considers a particle-hole excitation where the particle moves from site i to site j, the energy cost is $E_{+1,j} - E_{-1,i}$ if i and j are not nearest neighbors. On the other hand, if the particles are nearest neighbors (excitonic excitation), this costs

$$\Delta_{{\rm ph},ij} = U - V + W_j - W_i. \tag{100}$$

For the pure case, one thus sees from Eqs. (98) and (100) that the gap for creating a single-particle excitation is larger than for particle holes

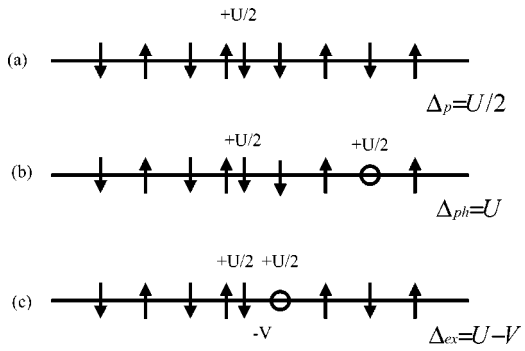

FIG. 15. Possible excitations in the atomic limit. Drawings are made for a chain for clarity, but the arguments are valid in arbitrary dimension d. (a) Energy cost to add one particle. (b) Generic particle-hole excitation. (c) Exciton, where the particle and the hole are on neighboring sites. In the presence of disorder the gap for excitonic excitations will close, first leading to the absence of a gap in the optical conductivity, but still to an incompressible system (see the text), leading to a Mott glass phase.

$$\Delta_{\rm p} = \frac{U}{2}, \tag{101}$$

$$\Delta_{\rm ex} = U - V; \tag{102}$$

this is the well-known excitonic binding that occurs in systems with a gap.

In the presence of disorder one can minimize the single-particle gap by choosing the site where the disorder potential is minimum, giving

$$\Delta_p = \frac{U}{2} + \frac{\min(W_i) - \max W_i}{2}, \tag{103}$$

where we choose $\overline{W_i} = 0$ for convenience. On the other hand, the minimal particle hole interaction corresponds to choosing the nearest neighbor pair $\langle i,j \rangle$ for which the difference in disorder potential is minimal:

$$\Delta_{\rm ex} = U - V - \min_{\langle i,j \rangle} |W_j - W_i|. \tag{104}$$

For an uncorrelated bounded disorder one has

$$\min(W_i) \sim -W, \tag{105}$$

$$\min(W_j - W_i) \sim -2W. \tag{106}$$

Thus, in the presence of a nearest-neighbor interaction V, the particle-hole gap closes faster, at $W_c = (U-V)/2$, when disorder increases, than the single-particle gap. For an homogeneous system this would simply signal an instability of the ground state. For a disordered system this need not be so, since only a fraction of the sites have their gap closing. Thus, in the presence of a small kinetic energy, the conductivity gap would close near this point, the compressibility remaining zero. Within this zero-kinetic-energy model one thus already finds three phases. The phase for which the particle-hole gap has closed for some sites but the single-particle gap is still finite can of course be identified with the Mott glass.

Thus the physics of the Mott glass, that has been derived for finite kinetic energy by the methods of the previous sections has its origin in excitonic effects. This is quite general, and does not rely on any special one-dimensional features. One dimension here was thus only a tool, allowing us to perform the calculation. We thus expect a Mott glass phase to be present in arbitrary dimension, and it would be interesting to check either through numerical calculations or mean-field methods whether one can recover the properties that we have identified here. The excitonic argument also shows clearly that some finite-range interaction is needed for a MG phase to appear. For a simple Hubbard model both the single-particle and particle-hole gap would close simultaneously (up to the distribution of disorder) and most likely the MG phase does not exist. In the presence of finite-range interactions the MG glass can be stabilized. A similar construction can be made for the spinless case, although it involves longer range (third-neighbor) interactions.

According to this physical picture of the MG phase, the low-frequency behavior of the conductivity is dominated by excitons (involving neighboring sites). This is at variance

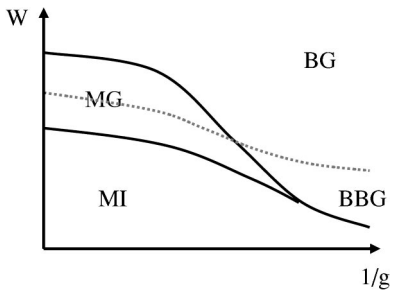

FIG. 16. Phase diagram of bosons in the limits $T \to 0$ and $\hbar \to 0$. W is the strength of the disorder, and g the amplitude of the commensurate potential for a fixed repulsive interactions. For weak disorder the boson system should retain a perfect topological order (i.e., no defects such as dislocations). Whether or not the line for which topological order is lost (dashed line) enters the MG phase is an open question. It is represented here for $d=3$. The incompressible phases are the Mott insulator (MI) or Mott glass (MG) phase. The compressible phases are either the Bragg Bose glass phase with perfect topological order (BBG), or the Bose glass (BG) phase if topological order is lost.

from the AG phase, where the particle and hole are created on distant sites. This has consequences on the precise low frequency form of the conductivity such as logarithmic corrections. In addition, since the excitons are neutral objects, although they can participate to the optical absorption, they need to be broken to give a dc current. One can thus give a naive estimate of the conductivity in the MG phase,

$$\sigma \sim n_{ex} e^{-V/T}, \tag{107}$$

where n_{ex} is the number of excitons in the ground state and V is the typical excitonic binding energy, which depends only weakly on the disorder.

2. Consequences for other systems

The above arguments also directly apply to other systems. In one dimension the spinless fermions can be mapped to a disordered spin systems. In this case the commensurate phase can either come from an antiferromagnetic staggered field, or more reasonably from a spin-Peierls distortion of the lattice. Such a perturbation would force the spin to lock into a singlet state. The disorder would be a random magnetic field.

Another system of interest is provided by hard core bosons. In one dimension, one can use exactly the phase Hamiltonian to represent interacting bosons,[14,24] but the excitonic arguments given in Sec. IV B 1 would also apply to interacting bosons in higher dimensions as well. In this case the Anderson glass phase becomes a Bose glass phase.[24,15] For classical systems the phase diagram is shown in Fig. 16. Even in the Bose glass phase, for weak disorder perfect topological order (stability to dislocations in the lattice) can persist in $d=3$, resulting in a Bragg Bose glass phase.[40,60] On the other hand, in any dimension the Mott insulator should exhibit perfect topological order. Thus an interesting and open issue is whether this topological order also subsist in at least a portion of the Mott glass phase.

V. CONCLUSION

In this paper, we have investigated the competition of a random and a commensurate potential. This question is relevant for host of physical systems, ranging from one-dimensional interacting fermions or bosons to classical systems in the presence of correlated disorder. The commensurate potential induces an incompressible Mott insulating phase with a gap in the conductivity. On the other hand, disorder induces a compressible Anderson insulating phase. While naive expectations predict a direct transition between these two phases, we find that if interactions are repulsive enough, an intermediate phase, the Mott glass phase, does exist. Although this phase is incompressible, like a Mott insulator phase, it does not have a gap in the optical conductivity, in a way similar to the Anderson insulator.

To obtain this phase we had to go beyond standard renormalization-group techniques which are perturbative in both commensurate and disorder potentials. We therefore used a bosonization associated with several nonperturbative techniques. The first one is a replica variational method, that allows for a complete calculation of the various physical observables such as the conductivity. The second method is a functional renormalization group approach, which is perturbative in $d=4-\epsilon$ dimensions and is well suited to study the transition from a Mott glass phase to a Mott insulator phase, as well as equivalent classical systems. In addition we have looked at the limit of zero kinetic energy, both for the bosonized Hamiltonian and directly on the fermion problem (both for the spinless problem and for the problem with spin). The latter yields a very general argument in favor of the existence of a Mott glass phase in any dimension. It also shows that the underlying mechanism for this phase is the creation of low-energy bound states (excitons) coming from the competition between interactions and disorder. These excitations play no role in the compressibility but contribute to the optical conductivity.

This phase could be observable in systems close to a metal-insulator transition, such as oxides, provided that one can measure simultaneously the optical conductivity and the compressibility. Numerical simulations for disordered boson systems could be prime candidates to observe this effect. Note that since all the phases have finite correlation lengths, this should be observable even in moderately small systems. Many problems remain open. In particular, it would be interesting to understand in detail the effect of a chemical potential on the Mott glass phase. Another open problem is the effect of temperature on the Mott glass phase. Finally, it would be interesting to investigate the possibility of aging dynamics in the Mott glass phase.

We thank R. Bhatt, S. Fujimoto, H. Fukuyama, A. Furusaki, L. Ioffe, C. Itoi, N. Nagaosa, Y. Suzumura, C. M. Varma and H. Yoshioka for discussions. E. O. acknowledges support from the NSF under Grant Nos. DMR 96-14999 and DMR 9976665 (during his stay at Rutgers University where part of this work was completed) and from Nagoya University.

APPENDIX A: FORWARD SCATTERING DISORDER AND PERIODIC POTENTIAL

In this appendix we examine the effects of the forward scattering disorder η, and neglect backward scattering altogether. For fermions, such an approximation is surely justified when $3/2<K<2$. Then the backward component of disorder is irrelevant and can be neglected. In the other case, $K<3/2$, backward scattering will be relevant, and drive the system into an Anderson glass state.

1. Solution of the variational equations

The action of the problem is

$$\frac{S}{\hbar}=\int dx\int_0^{\beta\hbar}d\tau\left[\frac{1}{2\pi K}\left\{v(\partial_x\phi)^2+\frac{(\partial_\tau\phi)^2}{v}\right\}-\frac{g}{\pi\alpha\hbar}\cos 2\phi-\frac{\mu(x)}{\pi\hbar}\partial_x\phi\right], \tag{A1}$$

which, after replication and average over disorder, gives

$$S_{\text{rep.}}=\sum_a\int dx\int_0^{\beta\hbar}d\tau\left[\frac{1}{2\pi K}\left\{v(\partial_x\phi_a)^2+\frac{(\partial_\tau\phi_a)^2}{v}\right\}-\frac{g}{\pi\alpha}\cos 2\phi_a\right]-\frac{D}{2(\pi\hbar)^2}\sum_{a,b}\int dx\times\int_0^{\beta\hbar}d\tau\int_0^{\beta\hbar}d\tau'\,\partial_x\phi_a(x,\tau)\partial_x\phi_b(x,\tau'). \tag{A2}$$

We use the GVM ansatz [Eq. (40)] with

$$vG_{ab}^{-1}(q,\omega)=\frac{[(vq)^2+\omega^2]}{\pi K}\delta_{ab}-\sigma_{ab}(q,\omega), \tag{A3}$$

as in the case of the backward scattering disorder. Using Eqs. (40) and (42), the variational energy F_{var} for the forward scattering problem is

$$F_{\text{var}}=\frac{1}{2\beta}\int\frac{dq}{2\pi}\sum_{n,a}\frac{\hbar}{\pi K}\left(vq^2+\frac{\omega_n^2}{v}\right)G_{aa}(q,\omega_n)-\frac{1}{2\beta}\int\frac{dq}{2\pi}\sum_{a,n}(\ln G)_{aa}(q,\omega_n)-\frac{g}{\pi\alpha}\sum_a\exp[-2\hbar G_{aa}(x=0,\tau=0)]-\frac{D}{2\pi^2\hbar}\sum_{a,b}\int\frac{dq}{2\pi}\hbar q^2G_{ab}(q,\omega_n=0). \tag{A4}$$

Minimizing Eq. (A4) with respect to $G(q,\omega)$ gives the variational equations

$$\sigma_{ab}(q,\omega_n)=-\frac{Dvq^2\beta}{\pi^2}\delta_{\omega_n,0}-\frac{4gv}{\pi\alpha}e^{-2\hbar G_{aa}(x=0,\tau=0)}\delta_{a,b}. \tag{A5}$$

It is easy to check that Eqs. (A5) only have replica-symmetric solutions in contrast to the case of backward scattering.

Using the standard techniques for inversion of matrices in the limit $n\to 0$,[42] one finds the following expressions for $G_c=G_{aa}+\Sigma_{b\neq a}G_{ab}$:

$$G_c(q,\omega_n)=\frac{v}{\frac{\hbar}{\pi K}(\omega_n^2+(vq)^2)+m^2}. \tag{A6}$$

For $G(q,\omega_n,u)$,

$$G(q,\omega_n,u)=\left(\frac{\pi\bar{K}}{\hbar}\right)^2\frac{Dq^2\beta\delta_{\omega_n,0}}{\pi^2v^2(q^2+\xi^{-2})^2}, \tag{A7}$$

where

$$m^2=\frac{4gv}{\pi\alpha}e^{-2\hbar G_{aa}(x=0,\tau=0)} \tag{A8}$$

and $\xi^2=v^2/(\pi\bar{K}m^2)$. One has

$$\lim_{\hbar\to 0,\bar{K}\text{fixed}}\hbar\tilde{G}(0,0)=\frac{\pi}{2}\frac{D\bar{K}^2}{v^2}\xi, \tag{A9}$$

leading to the self-consistent equation for ξ^2,

$$\left(\frac{l_1}{\xi}\right)^2\exp\left(\frac{\xi}{l_1}\right)=\left(\frac{l_1}{d}\right)^2, \tag{A10}$$

where we have defined $l_1^{-1}=D\bar{K}^2/(2v^2)$.

It is straightforward to show that Eq. (A10) has two solutions for $l_1/d>e/2$, and no solutions otherwise. In the first case, the solution with $l_1/\xi<1/2$ is a spurious solution, as can be seen by taking the limit of zero disorder ($l_1\to\infty$). Physically, the Mott gap is preserved (but reduced) as long as $l_1/d>e/2$, whereas for $l_1/d<1/2$ the Mott gap disappears. The transition gapped-gapless appears first order in the GVM, which is likely to be an artifact of the variational method. Note that the condition for the transition $l_1/d\sim e/2$ is in agreement with strong coupling extrapolations of the perturbative RG treatment.

2. Correlation functions

Another advantage of the GVM is to allow for a calculation of the correlation functions. Using Eq. (73), one sees that the density-density correlation function is given by

$$\overline{\langle T_\tau e^{i2\phi(x,\tau)}e^{\pm i2\phi(0,0)}\rangle}=e^{-\hbar[2\tilde{G}(0,0)\pm 2\tilde{G}(x,\tau)]}, \tag{A11}$$

which leads to

$$K_\perp(x,\tau)=\overline{\langle T_\tau\sin[2\phi(x,\tau)]\sin[2\phi(0,0)]\rangle}=e^{-\hbar 2\tilde{G}(0,0)}\sinh\hbar 2\tilde{G}(x,\tau), \tag{A12}$$

$$K_{\parallel}(x,\tau)=\overline{\langle T_\tau \cos[2\phi(x,\tau)]\cos[2\phi(0,0)]\rangle}$$
$$=e^{-\hbar 2\tilde{G}(0,0)}\cosh\hbar 2\tilde{G}(x,\tau). \quad \text{(A13)}$$

Since $\tilde{G}(x,\tau)=G_c(x,\tau)+G(x)$ and $\lim_{\hbar\to 0}\hbar G_c(x,\tau)=0$, only the static correlations survive. It is straightforward to show that

$$\lim_{\hbar\to 0,\overline{K}\text{fixed}} \hbar G(x)=\frac{1}{2}\left(\frac{\xi}{l_1}-\frac{|x|}{l_1}\right)e^{-|x|/\xi}, \quad \text{(A14)}$$

leading to the following expressions for the correlation functions:

$$K_\perp(x)=e^{-\xi/l_1}\sinh\left[\left(\frac{\xi}{l_1}-\frac{|x|}{l_1}\right)e^{-|x|/\xi}\right], \quad \text{(A15)}$$

$$K_{\parallel}(x)=e^{-\xi/l_1}\cosh\left[\left(\frac{\xi}{l_1}-\frac{|x|}{l_1}\right)e^{-|x|/\xi}\right]. \quad \text{(A16)}$$

It is easily seen that for $\xi<\infty$, $\lim_{x\to\infty}K_{\parallel}=e^{-\xi/l_1}$. In the absence of disorder, this limit would be exactly 1. Forward-scattering disorder thus leads to a reduction of the charge-density-wave long-range order. For $\xi\to\infty$, one recovers $K_{\parallel}(x)\sim e^{-|x|/l_1}$, a result that could have been derived directly.

APPENDIX B: SADDLE-POINT EQUATIONS

In this appendix we derive the saddle point equations obtained by minimizing the variational free energy [Eq. (42)]. Using Eqs. (42) and (39), we obtain

$$F_{\text{var}}=\frac{1}{2\beta}\int\frac{dq}{2\pi}\sum_{n,a}\frac{\hbar}{\pi K}\left(vq^2+\frac{\omega_n^2}{v}\right)G_{aa}(q,\omega_n)$$
$$-\frac{1}{2\beta}\int\frac{dq}{2\pi}\sum_{a,n}(\ln G)_{aa}(q,\omega_n)$$
$$-\frac{g}{\pi\alpha}\sum_a \exp[-2\hbar G_{aa}(x=0,\tau=0)]$$
$$-\frac{W}{(\pi\alpha)^2\hbar}\int_0^{\beta\hbar}d\tau\sum_{a,b}\exp\{-4\hbar[G_{aa}(x=0,\tau=0)$$
$$-G_{ab}(x=0,\tau)]\}. \quad \text{(B1)}$$

Varying in Eq. (B1) with respect to G, we obtain the following saddle-point equations:

$$G_c(q,\omega_n)^{-1}=\frac{\hbar}{\pi K}\left(vq^2+\frac{\omega_n^2}{v}\right)+\frac{4g}{\pi\alpha}\exp[-2\hbar G_{aa}(x=0,\tau=0)]+\frac{2W}{\hbar(\pi\alpha)^2}\int_0^{\beta\hbar}d\tau[1-\cos(\omega_n\tau)]$$
$$\times\left[e^{-4\hbar B_{aa}(x=0,\tau)}+\sum_{b\neq a}e^{-4\hbar B_{ab}(x=0,\tau)}\right], \quad \text{(B2)}$$

$$\sigma_{a\neq b}(q,\omega_n)=\frac{2Wv}{\hbar(\pi\alpha)^2}\int_0^{\beta\hbar}d\tau\cos(\omega_n\tau)\times\exp[-4\hbar B_{ab}(x=0,\tau)], \quad \text{(B3)}$$

with $G_c=G_{aa}+\Sigma_{b\neq a}G_{ab}$ and

$$B_{ab}(x,\tau)=G_{aa}(x,\tau)-G_{ab}(x,\tau). \quad \text{(B4)}$$

As was the case for fermions in a random potential,[20] one has $dB_{a\neq b}/d\tau=0$, leading to the following simplified expression of the replica off-diagonal self-energy:

$$\sigma_{a\neq b}=\frac{2Wv}{(\pi\alpha)^2}\beta\exp(-4\hbar B_{a\neq b})\,\delta_{\omega_n,0}. \quad \text{(B5)}$$

We still need to perform an analytical continuation from positive integer n to $n=0$ in Eqs. (B2) and (B3). In the GVM this is done assuming that for $n\to 0$, the G_{ab} become hierarchical matrices. Using the Parisi parametrization of hierarchical matrices in the $n\to 0$ limit.[42] Equations (B2) and (B3) give the equations

$$G_c^{-1}(q,\omega_n)=\frac{\hbar}{\pi K}\left(vq^2+\frac{\omega_n^2}{v}\right)+\frac{4g}{\pi\alpha}\exp[-2\hbar\tilde{G}(x=0,\tau=0)]+\frac{2W}{\hbar(\pi\alpha)^2}\int_0^{\beta\hbar}d\tau[1-\cos(\omega_n\tau)]$$
$$\times\left[\exp[-4\hbar\tilde{B}(x=0,\tau)]-\int_0^1 du\exp(-4\hbar B(u))\right], \quad \text{(B6)}$$

$$\sigma(q,\omega_n,u)=\frac{2Wv}{(\pi\alpha)^2}\beta\exp[-\hbar 4B(u)]\delta_{\omega_n,0}, \quad \text{(B7)}$$

where $u\in[0,1]$ is the Parisi parameter replacing the discrete replica index a.

APPENDIX C: SOLUTION OF RSB EQUATIONS

We want to solve the RSB saddle-point equations

$$vG_c^{-1}(q,\omega_n)=\frac{1}{\pi K}((vq)^2+\omega_n^2)+m^2+\sum_1(1-\delta_{n,0})+I(\omega_n), \quad \text{(C1)}$$

$$I(\omega_n)=\frac{2Wv}{(\pi\alpha v)^2\hbar}\int_0^{\beta\hbar}[e^{-4\hbar\tilde{B}(\tau)}-e^{-4\hbar B(u_c)}]\times[1-\cos(\omega_n\tau)]d\tau, \quad \text{(C2)}$$

$$\Sigma_1 = u_c[\sigma(u>u_c) - \sigma(u<u_c)], \tag{C3}$$

$$\sigma(u) = \frac{2Wv}{(\pi\alpha)^2} e^{-\hbar 4B(u)} \beta \delta_{n,0}, \tag{C4}$$

$$m^2 = \frac{4gv}{\pi\alpha} e^{-4\hbar\tilde{G}(0)}. \tag{C5}$$

Using the inversion formulas for hierarchical matrices,[42]

$$\tilde{G}(q,\omega_n=0) - G(q,\omega_n=0,u<u_c) = \frac{1}{G_c^{-1}(q,\omega_n=0)} + \left(1-\frac{1}{u_c}\right) \times \left(\frac{1}{G_c^{-1}(q,\omega_n=0) + \dfrac{\Sigma_1}{v}} - \frac{1}{G_c^{-1}(q,\omega_n=0)} \right), \tag{C6}$$

$$\tilde{G}(q,\omega_n=0) - G(q,\omega_n=0,u<u_c) = \frac{1}{G_c^{-1}(q,\omega_n=0) + \dfrac{\Sigma_1}{v}}, \tag{C7}$$

we obtain

$$B(u<u_c) = \frac{1}{\beta\hbar} \sum_{\omega_n} \int \frac{dq}{2\pi} G_c(q,\omega_n) + \frac{1}{\beta\hbar}\left(1-\frac{1}{u_c}\right) \int \frac{dq}{2\pi} \times \left(\frac{1}{G_c^{-1}(q,\omega_n=0) + \dfrac{\Sigma_1}{v}} - \frac{1}{G_c^{-1}(q,\omega_n=0)} \right), \tag{C8}$$

$$B(u>u_c) = \frac{1}{\beta\hbar} \sum_{\omega_n} \int \frac{dq}{2\pi} G_c(q,\omega_n) + \frac{1}{\beta\hbar} \int \frac{dq}{2\pi} \times \left[\frac{1}{G_c^{-1}(q,\omega_n=0) + \dfrac{\Sigma_1}{v}} - \frac{1}{G_c^{-1}(q,\omega_n=0)} \right]. \tag{C9}$$

Since

$$\lim_{\substack{\beta\to\infty \\ \hbar\to 0}} \frac{1}{\beta\hbar} \sum_{\omega_n} \int \frac{dq}{2\pi} G_c(q,\omega_n) = 0, \tag{C10}$$

we obtain

$$\lim_{\substack{\beta\to\infty \\ \hbar\to 0}} -\hbar B(u>u_c) = 0,$$

$$\lim_{\substack{\beta\to\infty \\ \hbar\to 0}} -4\hbar B(u<u_c) = 2\frac{\sqrt{\pi\bar{K}}}{\delta}\left[\frac{1}{(m^2+\Sigma_1)^{1/2}} - \frac{1}{m} \right]. \tag{C11}$$

Here we have assumed that when β goes to infinity, u_c goes to zero in such a way that $\beta u_c = \delta$ remains finite. Therefore,

$$\Sigma_1 = \frac{2W}{(\pi\alpha)^2} \delta v [1 - e^{2(\sqrt{\pi\bar{K}}/\delta)\{[1/(m^2+\Sigma_1)^{1/2}] - (1/m)\}}]. \tag{C12}$$

Next we derive a self-consistent equation for m by taking the $\hbar\to 0$ limit of the equation:

$$m^2 = \frac{4gv}{\pi\alpha} e^{-2\hbar\tilde{G}(0)}. \tag{C13}$$

We use first the general inversion formula[42]

$$\tilde{G}(q,\omega_n) = \frac{1}{G_c^{-1}(q,\omega_n)} \left[1 - \int_0^1 \frac{du}{u^2} \frac{[G^{-1}](u)}{G_c^{-1} - [G^{-1}](u)} - \frac{G^{-1}(0)}{G_c^{-1}} \right](q,\omega_n). \tag{C14}$$

In which we have

$$[G^{-1}](u<u_c) = 0, \tag{C15}$$

$$[G^{-1}](u>u_c) = \frac{-\Sigma_1}{v}, \tag{C16}$$

$$G^{-1}(0) = -\frac{\sigma(u<u_c)}{v}, \tag{C17}$$

so that

$$\tilde{G}(0,0) = \frac{1}{\beta\hbar} \int \frac{dq}{2\pi} \sum_{\omega_n} G_c(q,\omega_n) + \frac{1}{\beta\hbar} \int \frac{dq}{2\pi} \left[\frac{v\sigma(u<u_c)}{\left(\dfrac{\hbar}{\pi K}(vq)^2 + m^2 \right)^2} + \left(1-\frac{1}{u_c}\right) \times \frac{v\Sigma_1}{\left(\dfrac{\hbar}{\pi K}(vq)^2 + m^2 \right)\left(\dfrac{\hbar}{\pi K}(vq)^2 + m^2 + \Sigma_1 \right)} \right], \tag{C18}$$

leading to the expression for m in the $\beta\to\infty$ limit:

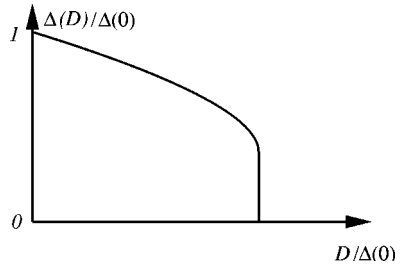

FIG. 17. The reduction of the gap with forward scattering disorder strength.

$$m^2=\frac{4gv}{\pi\alpha}\times\exp\left[2\frac{\Sigma_1(\pi\bar{K})^{1/2}}{\delta}\frac{1}{m(m^2+\Sigma_1)^{1/2}[m+(m^2+\Sigma_1)^{1/2}]}-\frac{W(\pi\bar{K})^{1/2}v}{(\pi\alpha)^2m^3}\exp\left(2\frac{\sqrt{\pi\bar{K}}}{\delta}\left[\frac{1}{(m^2+\Sigma_1)^{1/2}}-\frac{1}{m}\right]\right)\right]. \tag{C19}$$

A final equation for the breakpoint u_c is needed to close the system of equations. As discussed in Ref. 20, the physical choice corresponds to the so called marginality of the replicon condition which yields to $I(\omega_n)\propto|\omega_n|$ and to

$$\frac{4W(\pi\bar{K})^{1/2}v}{(\pi\alpha)^2(m^2+\Sigma_1)^{3/2}}=1. \tag{C20}$$

We use the quantities

$$m^2=\frac{v^2}{4\pi\bar{K}l_0^2}\mu^2, \tag{C21}$$

$$\Sigma_1=\frac{v^2}{4\pi\bar{K}l_0^2}\sigma_1, \tag{C22}$$

$$\frac{4\pi\bar{K}}{v\delta}=\eta, \tag{C23}$$

where l_0 and d are defined by Eqs. (51) and (52), respectively. The reduced variable μ is defined in such way that The point at which the replica symmetric solution becomes unstable has $\mu=1$ (see Fig. 17).

The self-consistent equations are rewritten

$$\sigma_1=\frac{2}{\eta}\left[1-\exp\left(\eta\frac{\mu-1}{\mu}\right)\right], \tag{C24}$$

$$\mu^2=4\left(\frac{l_0}{d}\right)^2 e^{[\eta(\mu-1)/\mu]-1/(2\mu^3)e^{\eta[(\mu-1)/\mu]}}, \tag{C25}$$

$$\mu^2+\sigma_1=1. \tag{C26}$$

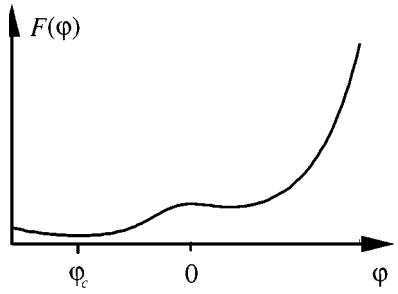

FIG. 18. The graph of $F(\varphi)$. Only the region with $\varphi<0$ is physical. F has a minimum for $\varphi=\varphi_c$. When $4(l_0/d)^2$ is smaller than $F(\varphi_c)$, Eq. (C28) has no solution.

To solve Eq. (C24) we introduce $\varphi=\eta(\mu-1)/\mu$. Physical solutions have $\eta>0$, $0\leqslant\mu\leqslant1$, and thus $\varphi\leqslant0$. Excluding the solution $\mu=1$ from Eq. (C24), we obtain the following equations in terms of φ:

$$\mu(\varphi)=\sqrt{\frac{1}{4}+2\frac{e^{\varphi}-1}{\varphi}}-\frac{1}{2}, \tag{C27}$$

$$4\left(\frac{l_0}{d}\right)^2=\mu^2(\varphi)\exp\left[-\frac{\varphi}{2}+\frac{e^{\varphi}}{2\mu^3(\varphi)}\right]=F(\varphi). \tag{C28}$$

We have thus reduced the self-consistent equations to a single equation for φ. Putting $\varphi=0$ in Eqs. (C27) and (C28), we obtain $\mu=1$ and recover condition (60) on d/l_0, i.e. the limit of validity of the RS solution. A plot of $F(\varphi)$ in shown in Fig. 18. As can be seen from this plot, F has a minimum for $\varphi=\varphi_c$. This implies that there can be no solution of Eqs. (C27) and (C28) when $l_0/d<\sqrt{F(\varphi_c)}/2$. The physical values of φ are thus located in the interval $[\phi_c,0]$. Numerically, it is found that $\varphi_c=-3.4325\pm0.0025$ and $F(\varphi_c)=1.15338$. The corresponding critical value of l_0/d is then $l_0/d=0.536977$ i.e. $d/l_0=1.86\ldots$.

APPENDIX D: FUNCTIONAL RENORMALIZATION-GROUP APPROACH

In this appendix we detail the analysis using the functional renormalization-group method of the effective model [Eq. (66)] in the presence of a mass term and correlated disorder in dimension d. We use the notations of the classical equivalent model [Eq. (22)]. The method is a Wilson momentum shell integration which it is an extension of Ref. 52 to the case of a finite mass $m^2>0$. Similar extensions can also be found in Refs. 55,56,53 and 61.

We start by studying $T_{cl}=0$. In the quantum problem this corresponds to the limit $K\to0$, $\hbar\to0$, and $\bar{K}=K/\hbar$ fixed [see Eq. (23)]. We consider a ground state which is τ independent $\phi(x,\tau)=\phi(x)$. It is in this limit that the GVM method revealed the presence of the Mott glass phase. It is more convenient to work with the function $\Delta(\phi)=-R''(\phi)$, where the bare $R(\phi)$ has been defined through Eq. (15). One first defines the running dimensionless disorder

$$\tilde{\Delta}_l(\phi)=\frac{A_d}{c^2}\Lambda_l^{d-4}\Delta_l(\phi), \tag{D1}$$

with $A_d=S_d/(2\pi)^d$, which is found to obey the $T_{cl}=0$ FRG equation:

$$\partial_l\tilde{\Delta}=\epsilon\tilde{\Delta}-f(l)\{(\tilde{\Delta}')^2+\tilde{\Delta}''[\tilde{\Delta}-\tilde{\Delta}(0)]\}, \tag{D2}$$

$$f(l)=\frac{1}{(1+\mu e^{2l})^2}, \quad \mu=m^2/\Lambda^2. \tag{D3}$$

The UV cutoff is reduced to $\Lambda_l=\Lambda e^{-l}$ ($\Lambda\sim 1/a$, where a is lattice constant). One can check that for $m=0$, Eq. (D2) reduces to the equation derived in Ref. 52. This equation turns out to be identical to the one describing point disorder in dimension d.

It is well known[52] that, in the case $m=0$ at $T=0$, a cusp develops at the origin for $l\to\infty$. One finds that $|\tilde{\Delta}(\phi,\infty)-\tilde{\Delta}(0,\infty)|\propto|\phi|$ for $\phi\to 0$. This implies that $\lim_{l\to+\infty}\tilde{\Delta}''(0,l)=-\infty$. It is thus important as a first step to analyze the cusp generation in the case $m\neq 0$. If we define $\Delta_2(l)=-\tilde{\Delta}''(0,l)$, we have, from Eq. (D2),

$$\partial_l\Delta_2=\epsilon\Delta_2+f(l)\Delta_2^2. \tag{D4}$$

This differential equation has, for a solution,

$$\frac{1}{\Delta_2(0)}-\frac{e^{\epsilon l}}{\Delta_2(l)}=\frac{1}{2}\int_1^{e^{2l}}dx\,\frac{1}{x^{(d-2)/2}(1+\mu x)^2}, \tag{D5}$$

where $\Delta_2(0)$ is the bare disorder. Introducing the Larkin length R_c in the absence of a mass ($\mu=0$), defined as the length scale at which Δ_2 diverges, i.e.,

$$\frac{1}{\Delta_2(0)}=\frac{1}{2}\int_1^{(R_c/a)^2}\frac{dx}{x^{(d-2)/2}}. \tag{D6}$$

One also obtains an equation that determines the Larkin length in the presence of a mass $\tilde{R}_c(\mu)$ defined as the length where $\Delta_2=+\infty$ for a nonzero μ as a function of R_c and μ:

$$\int_1^{(\tilde{R}_c/a)^2}\frac{dx}{x^{(d-2)/2}(1+\mu x)^2}=\frac{2}{4-d}\left[\left(\frac{R_c}{a}\right)^{4-d}-1\right]. \tag{D7}$$

Equation (D7) has two types of solutions, one with $\tilde{R}_c=\infty$ for weak disorder and another with $\tilde{R}_c<\infty$ for stronger disorder . As discussed in the text, this means that there are two phases: one in which disorder is strong enough to generate a cusp, and a second one in which the flow is cut by the presence of the mass before a cusp can be generated. The former corresponds to a Mott glass phase, while the second one corresponds to a Mott insulator phase. The equation of the transition line between these two phases is obtained by setting $\tilde{R}_c=\infty$ in Eq. (D7), and reads $R_c=R_c^*(\mu)$. At small μ and for $d<4$, we find that it behaves as

$$\frac{R_c^*(\mu)}{a}\sim\frac{C(d)}{\sqrt{\mu}}, \tag{D8}$$

where $C(d)$ is a dimension-dependent constant.

The physical quantity which is directly affected by the presence of the cusp is the tilt modulus $c_{44}(l)$. One finds that it satisfies the RG flow equation

$$\partial_l\ln c_{44}(l)=-\Delta_2(l)f(l), \tag{D9}$$

while c remains unrenormalized. This, clearly, either $\Delta_2(l)$ diverges sufficiently fast and $c_{44}(l=+\infty)=+\infty$ (interpreted as a Mott glass phase) or the mass cuts off the divergence early enough and $c_{44}(l=+\infty)$ remains finite (a Mott insulator phase). From the FRG approach, it is possible to compute the large l behavior of the tilt modulus exactly. For this, and to make further progress in the analysis of the two phases, we need to first consider the full flow of the function $\tilde{\Delta}_l(\phi)$. It can be shown easily that the solution of the flow equations at $\mu\neq 0$ can be obtained as a function of the solution at $\mu=0$ in the following ways:

$$\tilde{\Delta}_\mu(\phi,l)=h(l)\tilde{\Delta}_{\mu=0}[\phi,t(l)],$$

$$h(l)=\frac{e^{\epsilon l}}{1+\epsilon\int_0^l dl'\dfrac{e^{\epsilon l'}}{(1+\mu e^{2l'})^2}},$$

$$t(l)=\frac{1}{\epsilon}\ln\left(1+\epsilon\int_0^l\frac{e^{\epsilon l'}dl'}{(1+\mu e^{2l'})^2}\right), \tag{D10}$$

with the same initial condition. The behaviors at large l are

$$h(l)\sim e^{\epsilon[l-l_c^*(\mu)]}, \tag{D11}$$

$$t(l)\sim l_c^*(\mu), \tag{D12}$$

where $R_c^*(\mu)=ae^{l_c^*(\mu)}$ was defined above. From Eq. (D9) it is then easy to see that $c_{44}(l)=c_{44}(0)\Delta_2(l)/\Delta_2(0)e^{\epsilon l}$ which yields, e.g., $c_{44}(+\infty)$ in the no-cusp phase as

$$\frac{c_{44}(+\infty)}{c_{44}(0)}=\frac{\left(\dfrac{R_c}{a}\right)^\epsilon-1}{\left(\dfrac{R_c}{a}\right)^\epsilon-\left(\dfrac{R_c^*(\mu)}{a}\right)^\epsilon}. \tag{D13}$$

One thus finds that the renormalized tilt modulus diverges as one approaches the transition as

$$c_{44}(+\infty)\sim[R_c-R_c^*(\mu)]^{-1}. \tag{D14}$$

In $d=4$ one has, instead,

$$c_{44}(+\infty)=c_{44}(0)\frac{\ln(R_c/a)}{\ln[R_c/R_c^*(\mu)]}. \tag{D15}$$

In all cases one has $c_{44}(\infty)\to+\infty$ in the cusp phase. Conversely, in the no-cusp phase $c_{44}(\infty)$ remains finite. We ex-

pect that having $c_{44}(\infty)\to+\infty$ leads to no conductivity gap, but that having $c_{44}(\infty)<\infty$ produces a conductivity gap. In the cusp phase one can also expect that a term $|\partial_z u|$ is generated.[52] Such a term gives rise to the transverse Meissner effect. The critical field h_{c1} needed to bend vortices can be easily computed from the FRG approach.

We are now in position to estimate correlation functions in the case of point disorder or their z (i.e., τ) independent part in the case of correlated disorder (i.e., at $\omega_n=0$). One has

$$\overline{\langle\phi(q)\phi(-q)\rangle}=\tilde{\Gamma}(q)=e^{dl}\Gamma[qe^{l},\tilde{\Delta}(l),me^{2l}]. \tag{D16}$$

In the regime $qa\sim1$, the correlation function Γ can be obtained by perturbation theory in $\tilde{\Delta}$. Our strategy to obtain correlation functions[40] is therefore to integrate the RG equations until $qae^{l}\sim1$. At this point, we can calculate the correlation function Γ perturbatively and deduce $\tilde{\Gamma}$. We obtain

$$\tilde{\Gamma}(q)=\frac{\tilde{\Delta}[0,l=\ln(1/aq)]}{(aq)^{d-4}(q^2+m^2)^2}. \tag{D17}$$

Thus, for $d=2$, one obtains

$$\tilde{\Gamma}(q)=\frac{C}{q^2}q\gg m,$$

$$\tilde{\Gamma}(q)=\frac{C'}{m^4}q\ll m. \tag{D18}$$

Note that the *static* two point correlation functions or equivalently the correlations for point disorder do not exhibit a sharp transition.

It is crucial to check that the transition we found for $T_{cl}=0$ (i.e., $\hbar=0$) survives at finite temperature (finite $\hbar$). In the original quantum problem this corresponds to $K>0$ i.e., whether the intermediate phase exists for interactions that are not infinitely repulsive. The RG approach can be performed at finite T_{cl}. Introducing the effective running temperatures

$$\tilde{T}_l=T_{cl}\frac{A_d\Lambda_l^{d-1}}{2\sqrt{cc_z(l)}}k(l), \tag{D19}$$

$$k(l)=(1+\mu e^{2l})^{-1/2}, \tag{D20}$$

one finds that the FRG equation becomes

$$\partial_l\tilde{\Delta}=\epsilon\tilde{\Delta}+\tilde{T}_l\tilde{\Delta}''-f(l)\{(\tilde{\Delta}')^2+\tilde{\Delta}''[\tilde{\Delta}-\tilde{\Delta}(0)]\}. \tag{D21}$$

Note that in the quantum parameters $\tilde{T}_0\sim K$.

In the absence of a mass, $\mu=0$, it is easy to see[53] that the temperature $\tilde{T}_l$ runs to exactly zero at a finite length scale $l^*(\tilde{T}_0)-l_c\sim c(d)\tilde{T}_0$ for small $\tilde{T}_0$ with $l_c=\ln(R_c/a)$ the Larkin scale. This is because for $l>l_c$ the cusp is rounded[55,56] at finite $\tilde{T}_l$ with

$$\Delta_2(l)\sim\frac{\Delta^{*\prime}(0^+)^2}{\tilde{T}_l}\sim\chi\epsilon^2\frac{1}{\tilde{T}_l}, \tag{D22}$$

where $\Delta^*(\phi)$ is the $T=0$ fixed-point function, and χ a numerical constant. Thus one can write

$$\partial_l\ln\tilde{T}_l=1-d-\frac{1}{2}\partial_l\ln c_z(l) \tag{D23}$$

$$=1-d-\chi\epsilon^2\frac{1}{\tilde{T}_l}. \tag{D24}$$

This yield that $\partial_l\tilde{T}_l\approx-\chi\epsilon^2$ and thus the temperature vanishes beyond the scale $l^*(\tilde{T}_0)-l_c\sim(1/\chi\epsilon^2)\tilde{T}_0$.

It is thus clear that if μ is small enough so that $l^*(\tilde{T}_0)\ll l_c^*(\mu)$ introduced above, the temperature will vanish before the term $f(l)$ starts to deviate from 1, and change the behavior of the solutions. Thus at small nonzero temperature the divergence of c_{44} is not suppressed and the transition survives.

A more detailed analytical study can be performed by noting that the relation between the solution at finite μ and zero mass,

$$\tilde{\Delta}_{\mu,\tilde{T}_l}(\phi,l)=h(l)\tilde{\Delta}_{\mu=0,\hat{T}_l}[\phi,t(l)], \tag{D25}$$

with the same functions $h(l)$ and $t(l)$ as above and $\hat{T}_l=\tilde{T}_l/[h(l)f(l)]$. This confirms the above conclusions, but will not be detailed here.

Note, finally, that the above RG procedure assumes that the thickness L is constant. Since $\hbar$ runs to zero, this means that β runs to infinity; thus the temperature is also irrelevant in the quantum system.

*Electronic address: giam@lps.u-psud.fr
†Electronic address: ledou@lpt.ens.fr
‡Electronic address: edmond.orignac@lpt.ens.fr

[1] C. Monthus, O. Golinelli, and T. Jolicoeur, Phys. Rev. B **58**, 805 (1998).
[2] M. Azuma *et al.*, Phys. Rev. B **55**, 8658 (1997).
[3] M. Mori and H. Fukuyama, J. Phys. Soc. Jpn. **65**, 3604 (1996).
[4] R. Shankar, Int. J. Mod. Phys. B **4**, 2371 (1990).
[5] S. Fujimoto and N. Kawakami, Phys. Rev. B **54**, R11 018 (1996).
[6] E. B. Kolomeisky, Phys. Rev. B **48**, 4998 (1993).
[7] N. Kawakami and S. Fujimoto, Phys. Rev. B **52**, 6189 (1995).
[8] E. Orignac and T. Giamarchi, Phys. Rev. B **56**, 7167 (1997).
[9] E. Orignac and T. Giamarchi, Phys. Rev. B **57**, 5812 (1998).
[10] E. Orignac and T. Giamarchi, Phys. Rev. B **57**, 11 713 (1998).
[11] S. Fujimoto and N. Kawakami, Phys. Rev. B **56**, 9360 (1997).
[12] L. P. Regnault, J. P. Renard, G. Dhalenne, and A. Revcolevschi, Europhys. Lett. **32**, 579 (1995).
[13] B. Grenier, J. Renard, P. Veillet, C. Paulsen, R. Calemczuk, G. Dhalenne, and A. Revcolevschi, Phys. Rev. B **57**, 3444 (1998).
[14] F. D. M. Haldane, Phys. Rev. Lett. **47**, 1840 (1981).
[15] M. P. A. Fisher, P. B. Weichman, G. Grinstein, and D. S. Fisher, Phys. Rev. B **40**, 546 (1989).

[16] T. Giamarchi, Phys. Rev. B **46**, 342 (1992).
[17] T. Giamarchi, Physica B **230-232**, 975 (1997).
[18] D. R. Nelson and V. M. Vinokur, Phys. Rev. B **48**, 13 060 (1993).
[19] G. Blatter, M. V. Feigel'man, V. B. Geshkenbein, A. I. Larkin, and V. M. Vinokur, Rev. Mod. Phys. **66**, 1125 (1994).
[20] T. Giamarchi and P. Le Doussal, Phys. Rev. B **53**, 15 206 (1996).
[21] G. Grüner, *Density Waves in Solids* (Addison-Wesley, Reading, MA, 1994).
[22] A. Luther and V. J. Emery, Phys. Rev. Lett. **33**, 589 (1974).
[23] T. Giamarchi, Phys. Rev. B **44**, 2905 (1991).
[24] T. Giamarchi and H. J. Schulz, Phys. Rev. B **37**, 325 (1988).
[25] E. Orignac, T. Giamarchi, and P. L. Doussal, Phys. Rev. Lett. **83**, 2378 (1999).
[26] J. Sólyom, Adv. Phys. **28**, 209 (1979).
[27] V. J. Emery, in *Highly Conducting One-dimensional Solids*, edited by J. T. Devreese *et al.* (Plenum Press, New York, 1979), p. 247.
[28] H. J. Schulz, in *Mesoscopic Quantum Physics, Les Houches LXI*, edited by E. Akkermans, G. Montambaux, J. L. Pichard, and J. Zinn-Justin (Elsevier, Amsterdam, 1995), p. 533.
[29] J. Voit, Rep. Prog. Phys. **58**, 977 (1995).
[30] H. Maurey and T. Giamarchi, Phys. Rev. B **51**, 10 833 (1995).
[31] H. J. Schulz, Phys. Rev. Lett. **71**, 1864 (1993).
[32] F. Mila and X. Zotos, Europhys. Lett. **24**, 133 (1993).
[33] K. Sano and Y. Ōno, J. Phys. Soc. Jpn. **63**, 1250 (1994).
[34] V. L. Berezinskii, Zh. Éksp. Teor. Fiz. **65**, 1251 (1973) [Sov. Phys. JETP **38**, 620 (1974)].
[35] A. A. Abrikosov and J. A. Rhyzkin, Adv. Phys. **27**, 147 (1978).
[36] W. Apel, J. Phys. C **15**, 1973 (1982).
[37] T. Giamarchi and E. Orignac, cond-mat/0005220 (unpublished); to be published by Springer in *Theoretical Methods for Strongly Correlated Electrons*, CRM Series in Mathematical Physics.
[38] R. Chitra, T. Giamarchi, and P. Le Doussal, Phys. Rev. Lett. **80**, 3827 (1998).
[39] R. Chitra, T. Giamarchi, and P. Le Doussal (2001), cond-mat/0103392 (unpublished).
[40] T. Giamarchi and P. Le Doussal, Phys. Rev. B **52**, 1242 (1995).
[41] H. Fukuyama, J. Phys. Soc. Jpn. **45**, 1474 (1978).
[42] M. Mézard and G. Parisi, J. Phys. I **1**, 809 (1991).
[43] S. F. Edwards and P. W. Anderson, J. Phys. F: Met. Phys. **5**, 965 (1975).
[44] E. I. Shakhnovich and A. M. Gutin, J. Phys. A **22**, 1647 (1989).
[45] D. S. Fisher, Phys. Rev. B **31**, 7233 (1985).
[46] D. S. Fisher, Phys. Rev. Lett. **56**, 1964 (1986).
[47] L. Balents and D. S. Fisher, Phys. Rev. B **48**, 5949 (1993).
[48] L. Balents, J. P. Bouchaud, and M. Mézard, J. Phys. I **6**, 1007 (1996).
[49] T. Emig and T. Nattermann, Phys. Rev. Lett. **79**, 5090 (1997).
[50] T. Emig and T. Nattermann, Phys. Rev. Lett. **81**, 1469 (1998).
[51] T. Emig and T. Nattermann, Eur. Phys. J. B **8**, 525 (1999).
[52] L. Balents, Europhys. Lett. **24**, 489 (1993).
[53] P. Chauve, P. Le Doussal, and T. Giamarchi, Phys. Rev. B **61**, R11 906 (2000).
[54] P. Chauve, Ph.D. thesis, Paris XI University, 2000.
[55] P. Chauve, T. Giamarchi, and P. Le Doussal, Europhys. Lett. **44**, 110 (1998).
[56] P. Chauve, T. Giamarchi, and P. Le Doussal, Phys. Rev. B **62**, 6241 (2000).
[57] J. P. Bouchaud and A. Georges, Phys. Rev. Lett. **68**, 3908 (1992).
[58] V. M. Vinokur, M. B. Mineev, and M. V. Feigel'man, Zh. Éksp. Teor. Fiz. **81**, 2142 (1981) [Sov. Phys. JETP **54**, 1138 (1981)].
[59] B. I. Shklovskii and A. L. Efros, Zh. Éksp. Teor. Fiz. **89**, 406 (1098) [Sov. Phys. JETP **54**, 218 (1981)].
[60] T. Giamarchi and P. Le Doussal, Phys. Rev. B **55**, 6577 (1997).
[61] P. Chauve and P. Le Doussal, Phys. Rev. E **64**, 051102 (2001).
[62] In a previous publication, we used a slightly different definition for l_0 which led to different values of l_0/d.